DOI: 10.1534/genetics.109.106385

Chromosome Aberrations Resulting From Double-Strand DNA Breaks at a Naturally Occurring Yeast Fragile Site Composed of Inverted Ty Elements Are Independent of Mre11p and Sae2p

Anne M. Casper,[1] Patricia W. Greenwell, Wei Tang and Thomas D. Petes

Department of Molecular Genetics and Microbiology, Duke University Medical Center, Durham, North Carolina 27710

Manuscript received June 17, 2009
Accepted for publication July 18, 2009

ABSTRACT

Genetic instability at palindromes and spaced inverted repeats (IRs) leads to chromosome rearrangements. Perfect palindromes and IRs with short spacers can extrude as cruciforms or fold into hairpins on the lagging strand during replication. Cruciform resolution produces double-strand breaks (DSBs) with hairpin-capped ends, and Mre11p and Sae2p are required to cleave the hairpin tips to facilitate homologous recombination. Fragile site 2 (FS2) is a naturally occurring IR in *Saccharomyces cerevisiae* composed of a pair of Ty1 elements separated by ~280 bp. Our results suggest that FS2 forms a hairpin, rather than a cruciform, during replication in cells with low levels of DNA polymerase. Cleavage of this hairpin results in a recombinogenic DSB. We show that DSB formation at FS2 does not require Mre11p, Sae2p, Rad1p, Slx4p, Pso2p, Exo1p, Mus81p, Yen1p, or Rad27p. Also, repair of DSBs by homologous recombination is efficient in *mre11* and *sae2* mutants. Homologous recombination is impaired at FS2 in *rad52* mutants and most aberrations reflect either joining of two broken chromosomes in a "half crossover" or telomere capping of the break. In support of hairpin formation precipitating DSBs at FS2, two telomere-capped deletions had a breakpoint near the center of the IR. In summary, Mre11p and Sae2p are not required for DSB formation at FS2 or the subsequent repair of these DSBs.

PALINDROMES (inverted repeats with no spacer between the repeats) and inverted repeats separated by a short spacer ("IRs") are hotspots for genetic instability. In bacteria and yeast, palindromes and IRs are frequently deleted (Collins *et al.* 1982; Dasgupta *et al.* 1987; Gordenin *et al.* 1993; Ruskin and Fink 1993), and double-strand breaks (DSBs) and recombination are stimulated by these sequences (Farah *et al.* 2002, 2005; Lobachev *et al.* 2002; Lemoine *et al.* 2005; Cote and Lewis 2008; Eykelenboom *et al.* 2008). A palindrome introduced as a mouse transgene is a target for deletions and rearrangements and simulates gene conversion (Collick *et al.* 1996; Akgun *et al.* 1997). In human cells, the center of a large palindromic AT-rich repeat (PATRR) at 22q11.2 is a hotspot for breaks, translocations, and deletions and drives the most commonly observed non-Robertsonian translocation to 11q23, which also has a PATRR (Kurahashi *et al.* 2006, 2007; Kogo *et al.* 2007). IRs are also associated with gene amplification in human cancer cells (Tanaka *et al.* 2005, 2007) and in yeast (Narayanan *et al.* 2006).

The formation of cruciform or hairpin secondary structures at DNA palindromes and spaced IRs is believed to precipitate the DSBs and genetic instability at these regions. The likelihood that a perfect palindrome will extrude in a cruciform (Figure 1, left-hand side) is affected by base composition at the center of the palindrome and by arm length. Centers with AT base pairs are more likely to extrude than GC centers, presumably due to the easier melting of AT base pairs (Courey and Wang 1988; Zheng and Sinden 1988). Longer arm lengths increase the propensity for stable cruciform formation in both perfect palindromes and IRs (Sinden *et al.* 1991; Kogo *et al.* 2007). In plasmids or phage maintained in *Escherichia coli*, IRs with short spacers of 10 bp often adopt a cruciform secondary structure, but IRs with spacers >20 bp rarely extrude as cruciforms (Sinden *et al.* 1991; Allers and Leach 1995; Kogo *et al.* 2007). However, IRs with large spacers can form hairpins on single-stranded DNA (Figure 1, right-hand side), such as within the Okazaki fragment initiation zone on the lagging strand during DNA replication (Trinh and Sinden 1991; Voineagu *et al.* 2008).

We previously identified a naturally occurring fragile site in *Saccharomyces cerevisiae* (fragile site 2, FS2) that is a spaced IR on chromosome III. FS2 consists of two 6-kb

Supporting information is available online at http://www.genetics.org/cgi/content/full/genetics.109.106385/DC1.

The microarray data discussed in this article have been deposited in the NCBI Gene Expression Omnibus (Edgar *et al.* 2002) and are accessible through GEO Series accession no. GSE16502 (http://www.ncbi.nlm.nih.gov/geo/query/acc.cgi?acc=GSE16502).

[1]*Corresponding author:* Department of Biology, 316 Mark Jefferson, Eastern Michigan University, Ypsilanti, MI 48197.
E-mail: anne.casper@emich.edu

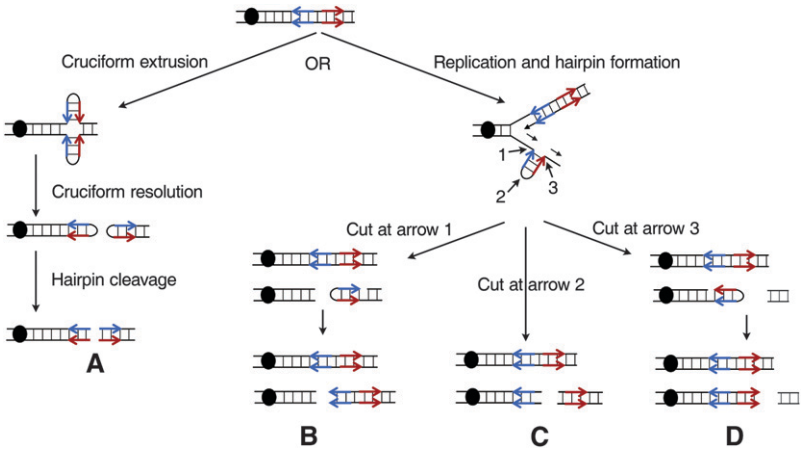

Figure 1.—Mechanisms of producing a recombinogenic DSB at an IR. The inverted repeat is shown as blue and red arrows, and each line represents a single DNA strand rather than duplicated chromatids. Labeled arrows show the positions of nuclease cleavage at the hairpin structure. The centromere is shown as a black oval. Only those broken DNA molecules containing a centromere are likely to produce a recoverable chromosome rearrangement. (A) Cruciform formation in a nonreplicating DNA molecule. Processing of the resulting structure by a resolvase would be expected to yield two hairpin-capped products that could be subsequently processed to yield uncapped broken DNA molecules. (B–D) DSBs produced by different positions of cleavage of the hairpin intermediate. We show hairpin formation associated with replication of the lagging strand. Cleavage at arrow 1 produces a capped hairpin in the acentric fragment or a centromere-containing fragment with a DSB proximal to FS2. Cleavage at arrow 2 results in a product in which the DSB is between the two elements of the inverted repeat. Cleavage at arrow 3 produces a capped hairpin or, if replication proceeds through the hairpin, results in a centromere-containing fragment with a DSB near the distal Ty element of FS2.

Ty1 elements in a head-to-head orientation separated by ~280 bp. Although this site is relatively inactive in wild-type cells, it is a hotspot for DSBs and translocations in cells with low levels of DNA polymerase α or δ (Lemoine *et al.* 2005, 2008). Polymerases α and δ, respectively, are the primase and replicative polymerase on the lagging strand. FS2-dependent DSBs have been physically observed by separating yeast chromosomes with **c**lamped **h**omogeneous **e**lectric **f**ield (CHEF) gel electrophoresis and using Southern blotting with chromosome III-specific probes. When cells have low levels of DNA polymerase α, a chromosome fragment of the size expected from a DSB at FS2 is observed. No such fragment is present in cells with wild-type levels of DNA polymerase α or in cells in which the centromere-proximal Ty1 of FS2 has been deleted, disrupting the potential for forming a secondary structure (Lemoine *et al.* 2005).

Our interpretation of these results is that the reduced level of polymerase α results in accumulation of single-stranded DNA on the lagging strand that permits the inverted Ty1 elements of FS2 to fold into a hairpin (Figure 1, right-hand side). Consistent with this suggestion, Voineagu *et al.* (2008) argue that the size of the Okazaki fragment initiation zone (OIZ) is a limiting factor in hairpin formation. Since the OIZ in eukaryotic cells is ~290 nucleotides (DePamphilis and Wassarman 1980; DePamphilis 2002), during normal DNA replication, the pairing of the FS2 Ty elements (separated by an ~280-bp spacer) will be very infrequent. The enlarged OIZ expected in cells with reduced polymerase α, however, could expose the IR regions flanking the spacer, allowing the formation of a DSB.

The DSB associated with FS2 had several different fates (Lemoine *et al.* 2005). Failure to repair the break resulted in loss of the broken chromosome. At low frequency, we observed strains with a stable terminal deletion, presumably representing "capping" of the broken chromosome by telomere repeats. A more frequent event was break-induced replication (BIR) between a Ty element of FS2 and a Ty or δ-element located on nonhomologous chromosomes, generating nonreciprocal translocations. δ-Elements are long terminal direct repeats ~330 bp in length located at the ends of Ty elements and are additionally present as "solo" elements scattered throughout the genome.

In addition to translocations that involve the Ty elements of FS2, we found translocations involving two directly repeated Ty elements located centromere-proximal to FS2; we termed this pair of elements FS1 (Lemoine *et al.* 2005). Most of the translocations that occur at FS1 are likely to be initiated by a DSB at FS2, since a deletion of one of the two FS2 Ty elements reduces the frequency of both FS2- and FS1-mediated events. Thus, we suggested that DSBs at FS2 are sometimes processed to generate a recombinogenic end in one of the Ty1 elements of FS1.

It has been proposed that cruciform structures are recognized and cleaved in the cell by a Holliday junction resolvase, resulting in two broken ends each capped with a hairpin. Cote and Lewis (2008) demonstrated that Mus81p was required for the resolution of a cruciform formed by a perfect palindrome carried on a plasmid in *S. cerevisiae*. In a study of an IR consisting of a pair of inverted human Alu elements separated by a 12-bp center spacer that was integrated on a yeast chromosome, however, Lobachev *et al.* (2002) found that Mus81p was not required for the formation of DSBs at the IR. In both of these studies, hairpin-capped breaks were demonstrated to be present at the center of symmetry, and Mre11p and Sae2p were required for repair of these breaks. In the absence of these proteins, DNA replication across the hairpin-capped sequence generated an extended inverted duplication, suggesting

that the essential function of Mre11p and Sae2p is to cleave the hairpin tip. Other studies have also implicated Mre11p and Sae2p in facilitating repair at perfect palindromes and at IRs with very short spacers in yeast (Rattray 2004; Farah *et al.* 2005; Rattray *et al.* 2005). Biochemical studies indicate that Mre11p, together with Sae2p, can cleave open small single-stranded DNA loops, such as those at the tips of hairpin-capped DSBs (Trujillo and Sung 2001; Lengsfeld *et al.* 2007). The previous studies of the effects of various mutants on the stability of inverted repeats have focused on sequences with the potential to extrude as a cruciform. Consequently, we investigated the roles of nucleases and recombination proteins on cleavage and DSB repair at FS2, which is likely to be extruded as a hairpin on the lagging strand rather than as a cruciform.

MATERIALS AND METHODS

Strain construction: All *GAL-POL1* strains in this study are isogenic with MS71, a *LEU2* derivative of AMY125 (*MAT*α *ade5-1 leu2-3 trp1-289 ura3-52 his7-2*) (Kokoska *et al.* 2000), except for changes introduced by transformation. All mating-type tester strains are isogenic with 1225 (*his4-15 leu2 thr4 ura3-52 trp1* Lys$^-$), except for changes introduced by transformation. Strain constructions and genotypes for all strains are in supporting information, Table S1.

Genetic methods and media: Transformation and mating methods were standard and all strains were grown at 30°. High-galactose medium contained 0.05% galactose and low-galactose medium contained 0.005% galactose, as well as 3% raffinose, plus the standard supplements of yeast extract and peptone; dextrose was omitted. Selective media were standard except for the addition of high or low galactose and the substitution of dextrose with raffinose (Guthrie and Fink 1991).

Quantitation of frequency of illegitimate mating: For each strain, we examined illegitimate mating in eight independent cultures. Each haploid *GAL-POL1 MAT*α experimental strain was grown overnight in 5 ml low galactose cultures. The mating tester strains (1225a and derivatives of 1225α) were grown overnight in rich growth medium (YPD). Cells were plated onto high galactose to assess viability, and $\sim 1 \times 10^6$ cells of the experimental strains were mixed with a fivefold excess of the tester. These mixtures were concentrated onto a sterile nitrocellulose filter and incubated on high galactose plates for 6 hr at 30°. The cells were rinsed from the filter with water and replated on diploid-selective medium. For legitimate mating, we plated a dilution of the mated cells. For illegitimate mating, the undiluted mixture was plated. After colony formation, we compared the number of diploids to the number of viable cells. Under these conditions, legitimate mating was very efficient, ≥90% in all strains except those with the *rad52* or *sae2* mutations. In these strains, the efficiency of legitimate mating was ~60%; the frequency of illegitimate mating was normalized to account for this decreased frequency of legitimate mating.

CHEF analysis, Southern blot analysis of illegitimate diploids, and analysis of DSBs on chromosome III: Genomic DNA was extracted in agarose plugs to avoid shearing, using the methods described by Lobachev *et al.* (2002). For CHEF analysis, electrophoresis was performed at 14° in a 1.0% gel, 0.5× TBE buffer in a Bio-Rad (Hercules, CA) CHEF Mapper XA. For analysis of chromosome III translocations in illegitimate diploids, yeast chromosomes were separated with switch times starting at 47 sec and extending to 2 min 49 sec at 5 V/cm for 33 hr. For analysis of the broken chromosome III in haploids with low levels of α-DNA polymerase, separation was done with switch times starting at 9.8 sec and extending to 34.92 sec at 6 V/cm for 18 hr 30 min.

For Southern blot analysis, we used a *CHA1* probe to the left arm of chromosome III (sequences 15,838–16,800) produced by PCR amplification of yeast genomic DNA. Probes were labeled by random-priming labeling, using Ready-To-Go DNA Labeling Beads (GE Healthcare). Southern hybridization and washing were standard. Membranes were exposed to a PhosphoImager screen for 1–3 days. Images were captured with a Typhoon imager (GE Healthcare) and quantification was performed using Quantity One analysis software (Bio-Rad).

All illegitimate diploids were initially characterized by CHEF gel separation of chromosomes followed by Southern blotting using the *CHA1* probe described above. Several illegitimate diploids were further analyzed using genomic microarrays and additional Southern blots as described by Lemoine *et al.* (2005). Details of the analysis of each illegitimate diploid are in File S1.

Telomere PCR: In several of the illegitimate diploids, we detected a chromosome III with terminal deletions. We expected that these chromosomes would be capped with telomeric repeats. From the CHEF gel and microarray analysis, two of these strains (PG297 and PG301) had deleted chromosomes with a breakpoint near the Ty elements of FS2. Using one primer that contained Ty1 sequences (Ty1-f: 5′-AAACGAATTCAGAGTTATTAGATGTGGATACATTGTGA) and one primer with telomere-related sequences (Telo-1-r: 5′-TAAAGCGGCCGCCGCGTCGACTAGTACCACCACACCCAC), we performed PCR using 50 ng of genomic DNA from PG297 or PG301, 35 pmol of each primer, 2.5 units of *Taq* DNA polymerase (Bioline), 200 μM each dNTP, 1.5 mM $MgCl_2$, and 5 μl of 10× buffer. The PCR conditions were 94° for 2 min followed by 35 cycles at 94° for 30 sec, 60° for 30 sec, and 72° for 4 min. The resulting PCR products were separated by gel electrophoresis and telomeric bands were excised, purified, and sequenced using the primers Ty1-seq1 (5′-GACCAACCAGATGGATTGGC), Ty1-seq2 (5′-CCTGACTCAGGTGATGGAGTG), Ty1-seq3 (5′-GACCCAGGTAGGTAGGAATTGAG), or ARB2-nr (5′-GGCCACGCGTCGACTAGTAC). This strategy for determining the site of telomere addition was based partly on primers designed by Schmidt *et al.* (2006).

RESULTS

Description of the experimental system: We previously showed that low levels of DNA polymerase α or δ result in elevated levels of genetic stability as monitored by the frequency of illegitimate mating (Lemoine *et al.* 2005, 2008). Mating between two *MAT*α strains is usually the consequence of loss of function of the *MAT*α locus from one of the two strains (Strathern *et al.* 1981). To analyze the various classes of genomic changes that lead to illegitimate mating, we used the system shown in Figure 2. The mating-type locus is located on the right arm of chromosome III. In one *MAT*α haploid strain (the experimental strain), the level of α-DNA polymerase is regulated by a galactose-inducible promoter (*GAL-POL1*) and the left and right arms of chromosome III contain the wild-type *HIS4* and *THR4* alleles, respectively. The tester *MAT*α strain has the *his4* and *thr4*

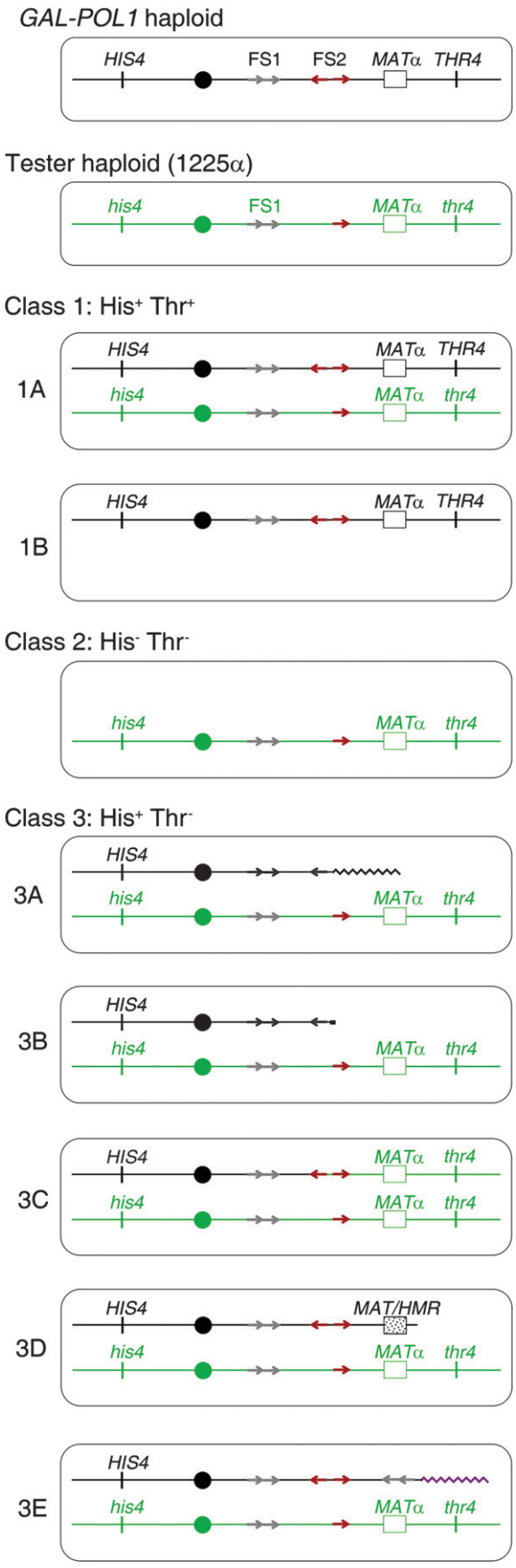

mutant alleles. In our previous study (Lemoine *et al.* 2005), we showed that growth of the *GAL-POL1* strain in medium containing 0.005% galactose and 2% raffinose (low galactose) resulted in very elevated (~200-fold) levels of illegitimate mating compared to the same strain grown in medium with 0.05% galactose and 2% raffinose (high galactose); the levels of α-DNA polymerase in these two types of medium are ~10% the wild-type level for the low galactose medium and threefold higher than the wild-type level for the high galactose medium (Lemoine *et al.* 2005).

In our previous study and in our present study, we observed diploids that were His^+ Thr^+ (class 1), His^- Thr^- (class 2), and His^+ Thr^- (class 3). Class 2 and 3 events are clearly the result of genetic instability in the low polymerase haploid because these events involve loss of markers from chromosome III in the *GAL-POL1* strain, but class 1 events may result from instability in either the *GAL-POL1* strain or the tester strain. On the basis of further analysis of the diploids by CHEF gels, microarrays, and other physical methods, some of these phenotypic classes can be subdivided. In class 1A diploids, the two chromosomes appear to be identical to the chromosomes of the two *MAT*α haploids. These diploids could represent rare fusions of two haploids of the same mating type without inactivation of *MAT*α information in either haploid, a point mutation within the *MAT*α locus, or a DSB in the tester strain repaired by a BIR event using the homolog derived from the *GAL-POL1* strain. Class 1B strains have only a single copy of chromosome III (by CHEF analysis) and, therefore, represent loss of a homolog from the tester strain. Class 2 strains have a single copy of chromosome III derived from the tester and thus represent loss of III from the experimental strain.

Figure 2.—Classes of illegitimate diploids induced by low levels of DNA polymerase α. In our experiments, a *GAL-POL1* *MAT*α *HIS4 THR4* haploid experimental strain was grown under conditions that result in low α-DNA polymerase. The strain was then mated to a tester strain (1225α) with the genotype *MAT*α *his4 thr4*. Ty elements are shown as red (FS2) or gray (FS1) arrows, with the orientation of the arrow representing the orientation of the Ty element. On the basis of the phenotypes of the resulting diploids, they were classified as class 1 (His^+ Thr^+), class 2 (His^- Thr^-), or class 3 (His^+ Thr^-). Subsequent analysis showed that there were two types of class 1 events. Class 1A events were a consequence of fusions between two *MAT*α strains without observed genomic changes; class 1B events were a consequence of loss of chromosome III from the tester strain. Class 2 events reflected loss of chromosome III from the experimental strain. The subclasses of class 3 were 3A (translocations with a breakpoint at FS1 or FS2 and at a Ty or δ-element on a nonhomologous chromosome), 3B (telomere-capped terminal deletion on the right arm of III), 3C (DSB on the right arm of III of the experimental strain, followed by repair from the homolog in the tester strain), 3D (deletion fusing *MAT* and *HMR*), and 3E (complex rearrangement with the FS2-centered palindrome described further in the text).

Class 3 diploids represent a more diverse class of chromosome rearrangements. Class 3A strains contain translocations that have the left arm of III, the centromere of III, and a portion of the right arm of III fused to sequences of a nonhomologous chromosome. The breakpoint of the translocation on III is usually within the centromere-proximal Ty element of FS2 and the breakpoint on the nonhomologous chromosome is also within a Ty element. We interpret these events as reflecting a DSB at FS2 that was repaired by a BIR event involving an ectopically located Ty element. In class 3B strains, one chromosome has a deletion of the right arm of III that removes the *MAT* locus and distal sequences. In class 3C strains, the two chromosomes appear to be similar to the chromosomes of the parental haploid strains except the mutant *thr4* marker is homozygous. Such strains likely reflect a DSB on III centromere-proximal to the mating-type locus of the experimental strain that was repaired by a BIR event using chromosome III of the tester strain after the mating. In class 3D strains, the chromosome derived from the experimental strain has an interstitial deletion that removes the *MAT* locus and the *THR4* gene as a consequence of recombination between the *MAT* locus and the silent mating-type information at *HMR*; deletions of this type were first observed by Hawthorne (1963). In class 3E strains, there is a duplication of the region located between FS1 and FS2 and deletion of the region distal to FS2 with a translocation at the breakpoint to a nonhomologous chromosome arm. As is discussed in detail later, the class 3E rearrangements result from DNA replication across a persistent "hairpin" structure at FS2, generating an extended inverted duplication centered at FS2.

We previously showed that elevated levels of classes 1–3 required both of the Ty elements composing FS2 *and* low levels of α-DNA polymerase (Lemoine *et al.* 2005). We inferred that all of these events, therefore, were likely to reflect a structure-specific DSB formed at FS2 in strains with low levels of DNA polymerase, and different modes of repair of this DSB result in the different classes.

The frequency of illegitimate mating of cells with low levels of DNA polymerase α is not affected by *mre11-H125N* or *mre11*Δ: In our previous studies, the *GAL-POL1* experimental strain and the test strain were wild type for DNA repair/recombination functions. To determine what genes are required for the generation of DSBs at FS2 or their repair, we constructed *GAL-POL1* strains with mutations in various repair/recombination genes, beginning with *MRE11*. Mre11p is required for processing of hairpins associated with palindromic and spaced IR sequences (Lobachev *et al.* 2002; Rattray 2004; Rattray *et al.* 2005; Farah *et al.* 2005; Lengsfeld *et al.* 2007; Cote and Lewis 2008). It is generally thought that cruciform extrusion at these sequences, followed by symmetrical cleavage by a Holliday junction resolvase, results in a pair of hairpin-capped DSBs (reviewed in Lewis and Cote 2006). Mre11p, which can cut small DNA loops (Trujillo and Sung 2001; Lengsfeld *et al.* 2007), then cleaves the tips of these hairpins to produce a free 3′ end available for repair. The *mre11-H125N* mutant is deficient specifically in Mre11p endonuclease activity (Moreau *et al.* 1999), and this mutant is phenotypically identical to the *mre11* deletion in its failure to repair breaks at cruciforms and spaced IRs (Lobachev *et al.* 2002). Although the IR at FS2 is unlikely to extrude as a cruciform, given its large central spacer, it could form a hairpin on the lagging strand during DNA synthesis under conditions of low polymerase α, and the tip of this hairpin would be expected to be a substrate for Mre11p.

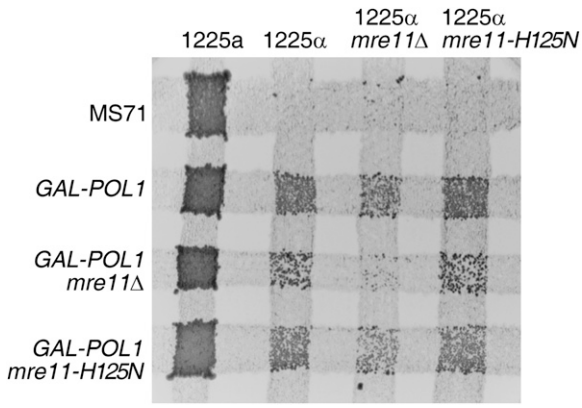

Figure 3.—Illegitimate matings in strains with *mre11* mutations: plate tests of legitimate and illegitimate mating. The *MAT*α wild-type parent strain (MS71) and isogenic *GAL-POL1*, *GAL-POL1 mre11*Δ, and *GAL-POL1 mre11-H125N* (a mutation eliminating the endonuclease activity of Mre11p; Moreau *et al.* 1999) strains were streaked on medium containing low levels of galactose (0.005%) (resulting in low levels of DNA polymerase α) and grown overnight. These strains were then mated by replica plating to four tester strains: 1225 *MAT***a**, 1225 *MAT*α, *mre11*Δ *MAT*α, and *mre11-H125N MAT*α. After the strains were allowed to mate overnight, they were replica plated to medium on which only diploids were capable of growth.

We created both *mre11*Δ and *mre11-H125N* mutants in our *GAL-POL1 MAT*α haploid strain and examined instability at FS2 in these mutants under low DNA polymerase conditions. Illegitimate mating was used as a general test of genetic instability at FS2 in these mutants as shown in Figure 3. After pregrowth on low galactose, illegitimate mating by *GAL-POL1 mre11-H125N* haploids was not substantially different from that of *GAL-POL1* haploids. Illegitimate mating was reduced in *GAL-POL1 mre11*Δ cells, however, particularly when the *MAT*α tester strain also carries an *mre11*Δ mutation. Using a tester strain carrying the same mutation as the *GAL-POL1* strain allows us to study not only the effect of the mutation on DSB formation at FS2, but also the effect of the mutation on repair of these breaks that can occur either before or after mating. We

TABLE 1

Illegitimate (α × α) mating of strains with low levels of α-DNA polymerase

Experimental genotype[a]	Test mater genotype[a]	Frequency of illegitimate mating ($\times 10^{-5}$)[b]	Frequency of class 1 ($\times 10^{-5}$)[c]	Frequency of class 2 ($\times 10^{-5}$)[c]	Frequency of class 3 ($\times 10^{-5}$)[c]
GAL-POL1	Wild type	360 (270–680)[d]	14	184	162
GAL-POL1	*mre11*Δ	148 (132–165)	73[e]	31	44
*GAL-POL1 mre11*Δ	*mre11*Δ	156 (138–174)	64[f]	39	53
GAL-POL1	*mre11-H125N*	223 (178–268)	13	95	115
GAL-POL1 mre11-H125N	*mre11-H125N*	140 (115–165)	6	60	74
GAL-POL1	*sae2*Δ	164 (137–191)	10	87	67
*GAL-POL1 sae2*Δ	*sae2*Δ	79 (59–99)	8	17	54
GAL-POL1	*rad52*Δ	170 (132–208)	29	39	102
*GAL-POL1 rad52*Δ	*rad52*Δ	40 (35–46)	14	25.5	0.5

[a] All experimental strains were isogenic with MS71, a *LEU2* derivative of AMY125 (*MAT*α *ade5-1 leu2-3 trp1-289 ura3-52 his7-2*) (Kokoska *et al.* 2000), except for the *GAL-POL1* gene and the indicated mutation. The mating-type tester strains are isogenic with 1225 (*MAT*α *his4-15 leu2 thr4 ura3-52 trp1 lys*) except for the indicated mutation.

[b] The frequency of illegitimate mating is corrected for viability and normalized to the level of legitimate mating. Numbers in parentheses indicate the 95% confidence interval from 8–10 different cultures.

[c] Fifty to 100 independent illegitimate diploids were examined for each mating to determine the relative frequencies of classes 1, 2, and 3.

[d] Values reported by Lemoine *et al.* (2005).

[e] Includes class 1B events (defined in Figure 2), which occurred at a frequency of 30×10^{-5}.

[f] Includes class 1B events (defined in Figure 2), which occurred at a frequency of 11×10^{-5}.

also observed that the viability of *mre11*Δ mutants was reduced in strains with low DNA polymerase α. After overnight growth in liquid medium with low galactose, only 9% of the *GAL-POL1 mre11*Δ haploids formed colonies, compared to 40 and 38% of *GAL-POL1 mre11-H125N* and *GAL-POL1* haploids, respectively.

Since this loss of viability would be expected to affect the efficiency of illegitimate mating, we normalized the frequency of illegitimate mating to the efficiency of legitimate mating between cells of the same genotype. Cells were pregrown in low galactose and then mated to a *MAT*α tester carrying the same *mre11* mutation as the *GAL-POL1* experimental strain. When corrected for viability and normalized to the frequency of legitimate mating, the average frequencies of illegitimate mating were similar in strains with and without Mre11p in the experimental strain (Table 1). We note, however, that the *mre11*Δ mutation in the *MAT*α tester strain reduced illegitimate mating to approximately half that of the *GAL-POL1* cells mated to a wild-type tester (Lemoine *et al.* 2005). Since cells lacking the Mre11p complex have increased sensitivity to DNA damaging agents, shortened telomeres, impaired DSB repair and checkpoint signaling, and increased chromosome loss (Tavassoli *et al.* 1995; Bressan *et al.* 1998; D'Amours and Jackson 2002; Krishna *et al.* 2007), it is likely that this inherent genetic instability in the *mre11*Δ tester strain may impair the ability of these cells to mate or to thrive after mating.

As described above, the phenotypes of the illegitimate diploids (His^+/His^-, Thr^+/Thr^-) can be used to divide them into three classes (Figure 2). Of 195 illegitimate diploids from mating of *GAL-POL1 mre11-H125N* cells to an *mre11-H125N* tester, classes 1, 2, and 3 were 4, 43, and 53%, respectively, which is a similar distribution to that seen for *GAL-POL1* cells mated to a wild-type tester (Lemoine *et al.* 2005). These percentages were multiplied by the frequency of illegitimate mating to generate the data for classes 1, 2, and 3 shown in Table 1. When either the *GAL-POL1* haploid or the *GAL-POL1 mre11*Δ haploid was mated to the *mre11*Δ tester, the frequency of class 1 events was substantially elevated relative to the other classes (Table 1).

In our previous studies mating the GAL-POL1 haploid to a wild-type tester, most class 1 diploids (His^+ Thr^+) had two normal-sized copies of chromosome III and could represent rare fusions between *MAT*α strains, point mutations in *MAT*α, or a DSB centromere-proximal to *MAT* in the tester strain that is repaired by BIR off the *GAL-POL1* chromosome III homolog. Since class 1 diploids do not sporulate and mate as *MAT*α strains (Lemoine *et al.* 2005), these diploids are not formed by mating-type switching. We sequenced the *MAT* locus in six class 1 strains derived from illegitimate mating between *GAL-POL1* haploids and a wild-type tester (DAMC590 to DAMC595). Sequencing results indicated six polymorphisms in this region between the two parent haploids (File S1 and Table S2). Of the six illegitimate diploids sequenced, five had both sequences derived from the parental haploids. Thus, these diploids appear to reflect rare fusions of *MAT*α haploids rather than point mutations inactivating the *MAT*α locus. One illegitimate diploid, DAMC593, was homozygous for all polymorphisms within the *MAT*α locus that were derived from the *GAL-POL1* haploid. Since CHEF gel analysis indicated that this illegitimate diploid contains two normal-sized chromosome IIIs, it is likely

that the DAMC593 strain was the result of a DSB centromere-proximal to the *MAT* locus in the tester that was repaired by BIR using the *GAL-POL1* chromosome III as a template.

Although class 1 events after mating to a wild-type tester are primarily rare fusions of *MAT*α haploids, our use of tester strains carrying nuclease mutations could potentially increase class 1 events resulting from instability of chromosome III in the tester haploid. For example, *mre11*Δ strains have been previously reported to have elevated chromosome loss (Bressan *et al.* 1998; Krishna *et al.* 2007). As noted above, the frequency of class 1 events was elevated in our analyses using the *mre11*Δ tester (Table 1). By quantitating the level of chromosome III *vs.* other chromosomes in CHEF gels, we found that 12 of 15 class 1 illegitimate diploids derived from a cross of *GAL-POL1 mre11*Δ cells to the *mre11*Δ tester had only a single copy of III, consistent with a high rate of chromosome loss in the tester (class 1B). Similarly, 10 of 17 class 1 illegitimate diploids from *GAL-POL1* cells mated to the *mre11*Δ were class 1B strains. In contrast, of 17 class 1 illegitimate diploids from *GAL-POL1* haploids mated to a wild-type tester strain, only one was haploid for III. The relative increase in class 1 diploids was observed only in matings using the *mre11*Δ tester and not the *mre11-H125N* tester. Thus, loss of chromosomes from the *mre11*Δ tester strain is not a consequence of loss of the nuclease activity of Mre11p.

DSB formation at FS2 resulting from low polymerase α is not significantly reduced in *mre11* mutants and in several other nuclease-deficient mutants: Since the majority of the DSBs on chromosome III in cells with low DNA polymerase α are at FS2 (Lemoine *et al.* 2005), we measured DSBs at FS2 in *mre11* mutant strains. Each strain was grown in high-galactose medium overnight and then incubated in medium with no galactose for 6 hr. We subsequently isolated genomic DNA and separated the chromosomes by CHEF gel electrophoresis, followed by Southern blotting with a probe on the left arm of chromosome III. We observed a DNA molecule of ~180 kb, the expected size for chromosome III broken at FS2, in the *GAL-POL1*, *GAL-POL1 mre11-H125N*, and *GAL-POL1 mre11*Δ cells (Figure 4). In all three of these strains, ~7% of the cells had a DSB at FS2 under these conditions. This fragment was not present in an isogenic wild-type strain (MS71) or in *GAL-POL1* cells with a deletion of the centromere-proximal Ty1 of FS2. The observation that Mre11p is not required for creating the DSB at FS2 is consistent with our observation that the frequency of illegitimate mating is relatively unaffected in *mre11* strains. We note that the broken III molecule in the *mre11*Δ strain appears smaller in comparison to the other strains (Figure 4). This altered migration could potentially be due to a difference in either telomere length or end resection of the DSB at FS2. Strains with the *mre11*Δ mutation have short telomeres (Moreau *et al.* 1999). Also, it has been

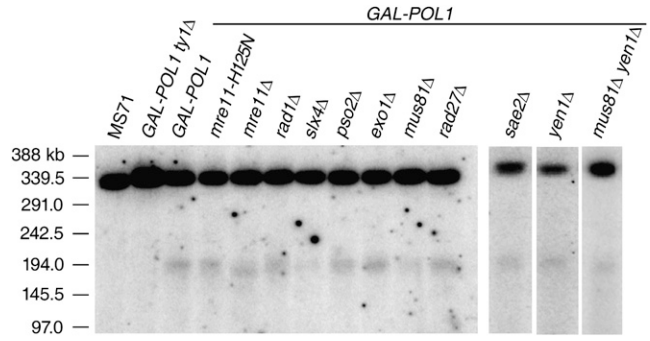

Figure 4.—Physical analysis of DSB formation at FS2 in strains deficient for various nucleases. All strains were grown overnight in high galactose medium and then washed in water and resuspended in medium lacking galactose for 6 hr. DNA was extracted and chromosomal DNA molecules were separated by gel electrophoresis as described in materials and methods. The separated molecules were examined by Southern analysis, using a probe derived from the left end of III. The ratio of chromosome III molecules broken at FS2 (180-kb fragment) *vs.* the intact III (330 kb) was quantitated using a PhosphoImager. MS71 is a wild-type haploid strain, and *GAL-POL1 ty1*Δ is isogenic with the *GAL-POL1* strain except that it lacks one of the two Ty1 elements that compose FS2 (Lemoine *et al.* 2005).

shown that Mre11p and Sae2p initiate end resection at induced DSBs, and although DSBs can still be resected in the absence of these proteins, this resection occurs more slowly (reviewed in Mimitou and Symington 2009). The *mre11-H125N* mutation does not affect either telomere length or DSB end resection (Moreau *et al.* 1999).

We also examined DSBs at FS2 in strains lacking various other nucleases (reviewed by Friedberg *et al.* 2006; Mimitou and Symington 2009; Rouse 2009) in the *GAL-POL1* background, including Exo1p (5′–3′ exonuclease and flap endonuclease), Mus81p (one subunit of a heterodimeric structure-specific nuclease), Pso2p (5′–3′ exonuclease), Rad1p (single-stranded endonuclease), Rad27p (5′–3′ exonuclease, 5′ flap endonuclease), Sae2p (single-stranded exonuclease), Slx4 (5′ flap endonuclease), and Yen1p (a Holliday junction-cleaving enzyme). Each mutant strain was analyzed for FS2-associated DSBs as described above. None of these nuclease mutants eliminated DSB formation at FS2. The ratio of DSB in each mutant strain to DSB in the *GAL-POL1* strain (normalized to the amount of intact chromosome III) and the 95% confidence limits, based on at least four measurements for each strain (except *rad52*), were as follows: *mre11-H125N*, 0.95 ± 0.16; *mre11*Δ, 1.37 ± 0.31; *sae2*, 1.07 ± 0.38; *rad1*, 0.58 ± 0.42; *slx4*, 0.57 ± 0.44; *pso2*, 1.12 ± 0.61; *exo1*, 1.15 ± 0.8; *mus81*, 1.04 ± 0.76; *rad27*, 0.94 ± 0.32; *yen1*, 1.58 ± 2.13; *mus81 yen1*, 0.77 ± 0.24; and *rad52*, 1.14. The ratio of DSBs in the *rad52* mutant was measured only once on a gel containing the *GAL-POL1* strain for comparison, but FS2-associated DSBs were also observed for this mutant in three other gels.

Mre11p is not required for the formation of FS2-associated translocations: We next investigated the various types of class 3 events (His^+ Thr^-) in *GAL-POL1-H125N* and *GAL-POL1 mre11*Δ cells. In our previous analysis of *GAL-POL1* cells, the most common types of class 3 events are class 3A (BIR resulting in nonreciprocal translocations), class 3B (terminal deletions), and class 3C (BIR events involving homologous chromosomes) (Lemoine *et al.* 2005). To subdivide the class 3 events in our present study, we first examined the sizes of chromosome III by CHEF gel electrophoresis, followed by Southern analysis using *CHA1* (a gene located on the left arm of III) as a hybridization probe. Illegitimate His^+ Thr^- diploids with two normal-sized copies of III were classified as 3C. Those strains with one normal III and one III of altered size were classified as either 3B or 3A, depending on the size of the alteration. The strains with an altered III of either 150 or 180 kb were considered class 3B, since they are the size expected for a telomere-capped break at FS1 or FS2, respectively; chromosome IIIs of any other size class were considered class 3A.

In *GAL1-POL1* illegitimate diploids, we previously reported a ratio of 3:1:4 for subclasses 3A:3B:3C (Lemoine *et al.* 2005). We did not observe any substantial deviations from this ratio in our analysis of *GAL-POL1* cells containing mutations in Mre11p. For *GAL-POL1 mre11-H125N* cells mated to the *mre11-H125N* tester, the ratio was 17:1:8 ($P = 0.31$). For *GAL-POL1 mre11*Δ cells mated to a wild-type tester, the ratio was 7:0:8 ($P = 0.59$), and when they were mated to an *mre11*Δ mutant tester, the ratio was 10:3:12 ($P = 0.99$). These data indicate that in all cases, the predominant classes are those that result from repair by BIR (classes 3A and 3C).

*Chromosome rearrangements in illegitimate diploids generated by mating GAL-POL1 mre11*Δ *cells to the mre11*Δ *tester strain:* We confirmed our classifications using DNA microarrays. Previously, we showed that class 3A events result in nonreciprocal translocations in which one breakpoint is in the centromere-proximal Ty of FS2 or one of the two Ty elements of FS1 and the other breakpoint is in a Ty element or a δ-element of a nonhomologous chromosome. Since the frequencies of translocations involving FS1 and FS2 are dependent on the FS2 pair of Ty elements (Lemoine *et al.* 2005), we suggested that these recombination events are initiated by a DSB that occurs between the Ty elements of FS2 as a consequence of hairpin formation. If the broken molecule is processed to a very limited extent, the Ty of FS2 can undergo a BIR event with a Ty element located on a nonhomologous chromosome, producing the translocation. If the broken chromosome is processed more extensively, then one of the Ty elements of FS1 can initiate the BIR event. The exposed Ty element then initiates a BIR event with a Ty or a δ-element on a nonhomologous chromosome (Figure 5). Almost all of the observed translocations involve Ty elements oriented in such a way that BIR produces a monocentric translocation. Presumably, BIR events that produce dicentric chromosomes or acentric fragments also occur but are selected against during the growth of cells containing the rearrangement. Class 3A events can be diagnosed by DNA microarrays because they result in a deletion of sequences from the right arm of III with a breakpoint in FS1 or FS2 and a duplication of sequences on a nonhomologous chromosome with a breakpoint at a mapped Ty or δ-element (Figure 5A). For some chromosome rearrangements, we used other techniques (Southern analysis or PCR) to confirm breakpoints (Figure 5C).

In four of the five class 3A illegitimate diploids we examined resulting from mating *MAT*α *GAL-POL1 mre11*Δ cells to a *MAT*α *mre11*Δ tester, there was a deletion of chromosome III with a breakpoint at FS1 or FS2 as well as amplification of another chromosome arm with a breakpoint at a Ty1 or a Ty2 element tester (Table 2 and File S1). In these four strains, the altered chromosome had the size expected for a BIR-mediated translocation (File S1). The complete analysis of one of these diploids (DAMC560) is shown in Figure 5. In one diploid (DAMC553), we observed a deletion of sequences distal to FS1, but no amplification. The observed chromosome size in this strain was ~240 kb, considerably larger that that expected for a simple deletion (class 3B). We did not attempt to characterize this rearrangement further.

Chromosome rearrangements in illegitimate diploids generated by mating GAL-POL1 mre11-H125N cells to the mre11-H125N tester strain: Eight independent class 3A illegitimate diploids were examined. The summary of this analysis is in Table 2 and the details of the analysis for each strain are in File S1. Five of the eight strains had the most common pattern observed in previous studies (Lemoine *et al.* 2005, 2008), deletion of chromosome III sequences beginning at FS1 or FS2 and amplification of sequences from a different homolog with a breakpoint in a Ty element. The three illegitimate diploids that did not fit this pattern were DAMC495, DAMC483, and DAMC476. The DAMC495 strain had a deletion of sequences distal to FS1 on chromosome III and amplification of sequences distal to *YBLWTy2-1* on chromosome II. The Ty elements were, however, in the wrong orientation to produce a monocentric translocation by BIR. One explanation of this result is that the yeast strains used in this study contained an unannotated Ty or δ; this rearrangement was not further analyzed. The DAMC483 diploid had two deletions. One deletion removed all of the sequences of chromosome III except those distal to *YCLWTy2-1*; this region of III has a cluster of transposable elements and was called the left arm hotspot (LAHS) by Warmington *et al.* (1986). The second deletion removed the sequences on chromosome II distal to *YBLWTy2-1*. Southern analysis

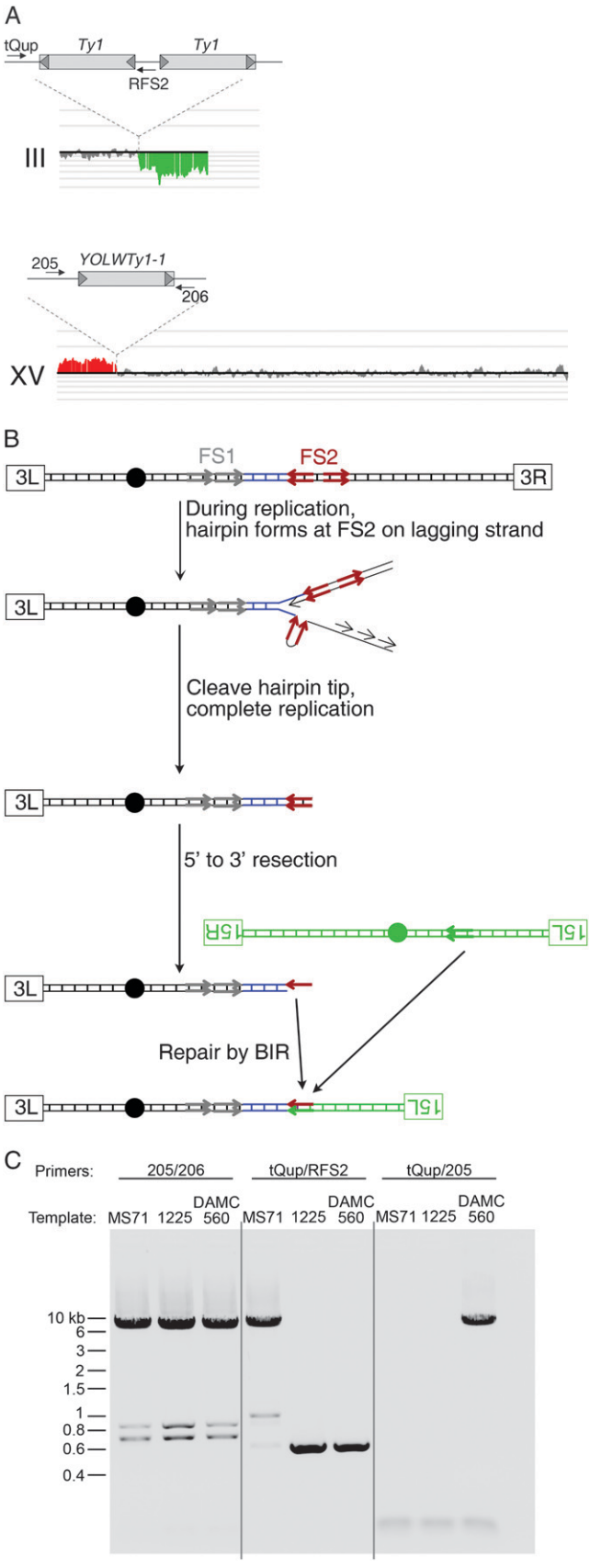

of this illegitimate diploid was consistent with the repair of two DSBs within these two Ty2 elements by single-strand annealing, resulting in a II–III translocation (File S1).

If the endonuclease function of Mre11p is required to cleave a hairpin-capped break at FS2, then we would expect that, in the absence of this protein, replication across hairpin-capped DSBs at FS2 would result in the formation of repair products with an extended inverted repeat centered at FS2, in a mechanism similar to that at the inverted Alu elements described by Narayanan *et al.* (2006). One of the *mre11-H125N/mre11-H125N* illegitimate diploids (DMAC476) had this pattern. This strain had a deletion on chromosome III of sequences distal to FS2, a duplication of chromosome III sequences between FS1 and FS2, and a duplication of chromosome XIV sequences distal to *YNLWTy1-2* (Figure 6A). Restriction digest mapping and Southern blot analysis of this illegitimate diploid determined that it had a palindromic amplification centered at FS2 and a translocation between the duplicated copy of FS1 centromere-distal to FS2 and *YNLWTy1-2* on chromosome XIV. This rearrangement is consistent with the formation of a dicentric chromosome centered at FS2 as a repair intermediate that is broken in or near FS1, followed by BIR-mediated repair of the broken end using a Ty element on chromosome XIV (Figure 6B and File S1). Although this chromosome is consistent with what we expect if the nuclease activity of Mre11p was required to process the spacer of the FS2-associated hairpin, several points should be emphasized. First, we found only

Figure 5.—Physical analysis of a translocation produced by a BIR event between nonallelic Ty elements in an *mre11*Δ/*mre11*Δ illegitimate diploid. (A) Microarray analysis. DNA was isolated from a class 3 illegitimate diploid (DAMC560) resulting from the mating of two *MAT*α *mre11*Δ strains. This sample was labeled with a Cy5 fluorescent nucleotide and mixed with a control DNA sample labeled with a Cy3 fluorescent nucleotide, and this mixture was used a hybridization probe of a microarray containing all of the yeast ORFs and intergenic regions. The ratios of hybridization are indicated as vertical lines with deletions and additions in the experimental strain shown in green and red, respectively (analysis by the CGH-Miner program). No changes were observed on chromosomes other than III and XV. The deletion breakpoint on III is at FS2, and the amplification breakpoint on XV is at *YOLWTy1-1*. Large gray rectangles represent Ty elements, short gray arrowheads show δ-elements, and small black arrows represent PCR primers. (B) Mechanism for generating the III–XV translocation by BIR. Centromeres are indicated by black circles, left and right telomeres are identified by labeled rectangles, and Ty elements are indicated by arrows. (C) Confirmation of translocation by PCR. The positions of the primers are shown in A. MS71 is the wild-type parental haploid from which all *GAL-POL1* experimental strains are derived, and 1225 is the wild-type parental haploid from which all mating-type tester strains are derived. MS71 has the centromere-distal Ty at FS2 that 1225 lacks. As expected, PCR using primers from III (tQup) and XV (205) generates a product when DNA from the strain with the III–XV translocation is used as a template.

TABLE 2

Chromosome III rearrangements in class 3 illegitimate diploids

Illegitimate diploid	Relevant genotype[a]	Subclass	Altered chromosome size (kb)[b]	Chromosome III alteration	Other chromosome alteration	Interpretation[c]
DAMC473	*mre11-H125N* / *mre11-H125N*	3A	436	Deletion of sequences distal to FS1	Amplification of right arm of X distal to *YJRWTy1-2*	BIR event
DAMC474	*mre11-H125N* / *mre11-H125N*	3A	300	Deletion of sequences distal to FS2	Amplification of right arm of V distal to *YERCTy1-1*	BIR event
DAMC475	*mre11-H125N* / *mre11-H125N*	3A	700	Deletion of sequences distal to FS1	Amplification of right arm of II distal to*YBRWTy1-2*	BIR event
DAMC476	*mre11-H125N* / *mre11-H125N*	3E	776	Amplification between FS1 and FS2; deletion of sequences distal to FS2	Amplification of left arm of XIV distal to *YNLWTy1-2*	Palindromic amplification between FS1 and FS2 along with BIR event
DAMC479	*mre11-H125N* / *mre11-H125N*	3A	250	Deletion of sequences distal to FS1	Amplification of right arm of I distal to *YARWdelta7*	BIR event
DAMC483	*mre11-H125N* / *mre11-H125N*	3A	850	Deletion of sequences distal to *YCLWTy2-1*	Deletion of left arm of II distal to *YBLWTy2-1*	Half crossover; repair by SSA of breaks at or near the repetitive elements involved
DAMC484	*mre11-H125N* / *mre11-H125N*	3A	813	Deletion of sequences distal to FS2	Amplification of right arm of IV distal to *YDRCTy1-2*	BIR event
DAMC485	*mre11-H125N* / *mre11-H125N*	3B	194	Deletion of sequences distal to FS2	None detected by genomic microarray	Telomere-capped break
DAMC495	*mre11-H125N* / *mre11-H125N*	3A	194	Deletion of sequences distal to FS1	Amplification of left arm of II distal to *YBLWTy2-1*	III/II translocation confirmed; wrong orientation of Ty elements for BIR
DAMC551	*mre11*Δ / *mre11*Δ	3A	2000	Deletion of sequences distal to FS2	Amplification of right arm of XII distal to rDNA array	BIR event, assuming Ty element present within rDNA array
DAMC552	*mre11*Δ / *mre11*Δ	3A	388	Deletion of sequences distal to FS2	Amplification of left arm of II distal to Watson Ty element near *YBLCdelta7* (not in sequenced strain)	BIR event
DAMC553	*mre11*Δ / *mre11*Δ	3A	242	Deletion of sequences distal to FS1	None detected by genomic microarray	Uncharacterized rearrangement; chromosome size inconsistent with telomere capping at FS1
DAMC555	*mre11*Δ / *mre11*Δ	3B	194	Deletion of sequences distal to FS2	None detected by genomic microarray	Telomere-capped break
DAMC560	*mre11*Δ / *mre11*Δ	3A	300	Deletion of sequences distal to FS2	Amplification of left arm of XV distal to *YOLWTy1-1*	BIR event
DAMC561	*mre11*Δ / *mre11*Δ	3A	700	Deletion of sequences distal to FS1	Amplification of right arm of II distal to *YBRWTy1-2*	BIR event
DAMC536	*sae2*Δ / *sae2*Δ	3A	300	Deletion of sequences distal to FS2	Amplification of right arm of V distal to *YERCTy1-1*	BIR event

(*continued*)

TABLE 2

(Continued)

Illegitimate diploid	Relevant genotype[a]	Subclass	Altered chromosome size (kb)[b]	Chromosome III alteration	Other chromosome alteration	Interpretation[c]
DAMC539	*sae2*Δ/*sae2*Δ	3A	400	Deletion of sequences distal to FS2	Amplification of left arm of II distal to Watson Ty element near *YBLCdelta7* (not in sequenced strain)	BIR event
DAMC547	*sae2*Δ/*sae2*Δ	3D	250	Deletion of sequences between *MAT* and *HMR*	None	Unequal crossover or SSA (HAWTHORNE deletion)
DAMC549	*sae2*Δ/*sae2*Δ	3A	250	Deletion of sequences distal to FS1	Amplification of left arm of VII distal to Crick Ty element near *YGRWdelta3* (not in sequenced strain)	BIR event
DAMC550	*sae2*Δ/*sae2*Δ	3A	440	Amplification between *YCRCdelta6* and FS1; deletion of sequences distal to FS2	Amplification of right arm of X distal to *YJRWTy1-1*	Palindromic amplification between *YCRCdelta6* and FS1 plus a BIR event
PG270	*rad52*Δ/*rad52*Δ	3A	654	Deletion of all III sequences except those centromere-distal to *YCLWTy2-1*	Deletion of right arm of VII distal to *YGRCTy2-1*	Half crossover, repair by SSA of breaks at or near the repetitive elements involved
PG271	*rad52*Δ/*rad52*Δ	3D	243	Deletion between *MAT* and *HMR*	None	Unequal crossover or SSA (Hawthorne deletion)
PG272	*rad52*Δ/*rad52*Δ	3A	218	Deletion of sequences distal to *YCR034W*	None	Size is consistent with repair by telomere addition
PG273	*rad52*Δ/*rad52*Δ	3A	218	Deletion of sequences distal to FS1	Deletion of left arm, centromere, and right arm of I up to *YARWdelta6*	Half crossover, repair by SSA of breaks at or near the repetitive elements involved
PG282	*rad52*Δ/*rad52*Δ	3A	218	Deletion of sequences distal to FS2	By genomic array, no other changes. By band array, left arm of II at *YBLWTy2-1* is attached to the broken III	Half crossover, repair by SSA of breaks at or near the repetitive elements involved
PG283	*rad52*Δ/*rad52*Δ	3A	267	Amplification of sequences distal to *YCLWTy2-1* and deletion of sequences distal to FS2	None	BIR

(*continued*)

TABLE 2

(Continued)

Illegitimate diploid	Relevant genotype[a]	Subclass	Altered chromosome size (kb)[b]	Chromosome III alteration	Other chromosome alteration	Interpretation[c]
PG284	*rad52Δ* / *rad52Δ*	3A	230	Deletion of sequences distal to FS2	Deletion of left arm, centromere, and right arm of I up to *YARCdelta8*	Half crossover, repair by SSA of breaks at or near the repetitive elements involved
PG286	*rad52Δ* / *rad52Δ*	3A	n/a	Monosomic for chromosome III	None	Repair by SSA of a break on III (centromere-proximal to FS2) in both the *GAL-POL1* haploid and the tester strain
PG297	*rad52Δ* / *rad52Δ*	3B	194	Deletion of sequences distal to FS2	None detected by genomic microarray	Telomere-capped break
PG298	*rad52Δ* / *rad52Δ*	3A	218	Deletion of all III sequences except those centromere-distal to *YCLWTy2-1*	Deletion of left arm of VI distal to *YFLWTy2-1*	Half crossover, repair by SSA of breaks at or near the repetitive elements involved
PG300	*rad52Δ* / *rad52Δ*	3A	557	Deletion of sequences distal to FS2	Deletion of left arm, centromere, and right arm of XII up to *YLRCdelta18*	Half crossover, repair by SSA of breaks at or near the repetitive elements involved
PG301	*rad52Δ* / *rad52Δ*	3B	194	Deletion of sequences distal to FS2	None detected by genomic microarray	Telomere-capped break

[a] Only the mutations that differ from the progenitor *GAL-POL1* strain and the mating-type tester are noted. All strains were derived from MS71 or 1225, as described in the Table 1 legend.

[b] The approximate sizes of the altered chromosome were estimated from a CHEF gel separation of chromosomes, followed by Southern blotting with a probe on the left arm of chromosome III.

[c] Details of the analysis of each illegitimate diploid are in File S1. All of the listed illegitimate diploids were analyzed by CHEF gel and microarray analysis; some were further examined by PCR and Southern analysis.

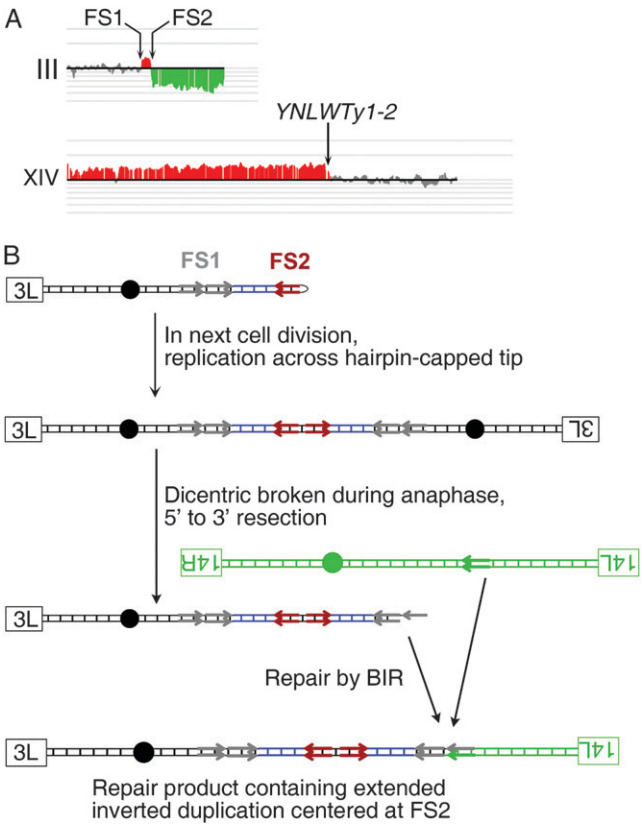

Figure 6.—Analysis of a chromosome rearrangement with a 20-kb palindrome centered on FS2 in an *mre11–H125N/mre11–H125N* illegitimate diploid (DAMC476). (A) Microarray analysis. The analysis was performed as described in Figure 5. On chromosome III, there was a deletion distal to FS2 and a duplication of the sequences between FS1 and FS2. The region of chromosome XIV distal to *YNLWTy1-2* was duplicated. Southern analysis (described in File S1) indicated the presence of a chromosome with a large palindrome centered on FS2. (B) Mechanism for generating a rearranged chromosome with an extended palindrome. Centromeres are indicated by black circles, left and right telomeres by labeled rectangles, and Ty elements by arrows.

one such rearrangement among 13 class 3A events in diploids homozygous for *mre11-H125N* or *mre11*Δ, indicating the cleavage of the associated hairpin is efficient in the absence of the Mre11p nuclease. Second, we previously observed a similar chromosome rearrangement in a wild-type *GAL-POL1* strain (Lemoine *et al.* 2005). In summary, the Mre11p endonuclease activity is not required to form the same types of translocations as observed in the wild-type strain.

We also used microarrays to analyze two illegitimate *mre11-H125N/mre11-H125N* diploids (DAMC485 and DAMC555) assigned to class 3B by CHEF and Southern analysis. This analysis confirmed that these diploids had a deletion of the sequences distal to FS2 on chromosome III with no additional changes (File S1).

*Chromosome rearrangements in illegitimate diploids generated by mating GAL-POL1 mre11-H125N or GAL-POL1 mre11*Δ *cells to a MRE11 tester strain:* We also analyzed 12 class 3A illegitimate diploids derived from mating *GAL-POL1 mre11-H125N* cells to a wild-type tester. All but one of these diploids had chromosome rearrangements consistent with the BIR event illustrated in Figure 5 (File S1). The exceptional diploid (DAMC461) had a chromosome III with a deletion of sequences distal to FS1 and an amplification of a 190-kb internal segment of VII. The size of the translocation was not consistent with a simple addition of the chromosome VII segment to the truncated chromosome III, and the rearranged chromosome was not further characterized (File S1). We also analyzed four class 3A illegitimate diploids resulting from mating *GAL-POL1 mre11*Δ cells to a wild-type tester. Three had the typical type of translocation of class 3A diploids, and one (DAMC461) had a complex chromosome rearrangement (File S1).

Sae2p is not required for the formation of FS2-associated translocations: Sae2p is a nuclease that cooperates with Mre11p in processing of short palindromes *in vitro* (Lengsfeld *et al.* 2007). This protein is also involved in the repair of breaks at palindromes and spaced IRs (Lobachev *et al.* 2002; Rattray 2004; Rattray *et al.* 2005; Cote and Lewis 2008). Recombinational repair at the Alu-IR generated by Lobachev *et al.* (2002) is equally defective in *mre11*Δ, *mre11-H125N*, and *sae2*Δ cells, and extended inverted duplications centered at the IR were observed in all of these mutants. We examined illegitimate mating, DSB formation at FS2, and chromosome rearrangements in illegitimate diploids in *sae2*Δ strains. As noted above, the amount of FS2-associated DSBs in *GAL-POL1 sae2*Δ cells after 6 hr growth in medium with no galactose was not appreciably different from that in cells with Sae2p (Figure 4).

The frequency of illegitimate diploids was reduced about twofold when both the experimental and the tester strain had the *sae2*Δ mutation (Table 1). Most of this reduction was in class 2 diploids, representing chromosome loss. Although the reason for this reduction is not clear, it is possible that *sae2*Δ haploids lacking chromosome III are less capable of being rescued by mating than *SAE2* strains. Unlike the *mre11*Δ tester strain, the *sae2*Δ mutation in the tester strain did not elevate the frequency of class 1 illegitimate diploids compared to crosses with a wild-type tester, indicating that genome instability in the *sae2*Δ tester does not substantially contribute to illegitimate mating. As before, we subdivided the class 3 illegitimate diploids by CHEF gel analysis followed by Southern blotting. Of 18 strains examined, the ratio of class 3A:3B:3C was 9:1:8, similar to that observed for the wild-type and *mre11* strains.

We analyzed five class 3A strains by microarrays (Table 2 and File S1). Three strains (DAMC536, DAMC539, and DAMC549) had nonreciprocal translocations with one breakpoint at FS1 and FS2 and a second within a Ty element on a nonhomologous chromosome. The strain DAMC547 had a deletion on the right arm of chromo-

some III between the *MAT* locus and *HMR*, likely as a result of unequal crossing over or single-strand annealing between these loci. The last illegitimate diploid, DAMC550, had a deletion of chromosome III distal to FS2, a duplication of chromosome III between *YCRC-delta6* and FS1, and a duplication on chromosome X distal to the tandem pair of Ty1 elements *YJRWTy1-1* and *YJRWTy1-2*. This set of alterations is consistent with a mechanism described by Vanhulle *et al.* (2007) in which a DSB at or distal to FS2 is extensively processed, allowing for pairing between the Ty elements of FS2 and FS1. DNA replication across this intermediate leads to the formation of a dicentric chromosome with an inverted duplication around FS1. This dicentric is broken during anaphase and repaired by BIR (Figure S1). Using restriction digest mapping, we confirmed there is an extended inverted duplication around FS1 in this illegitimate diploid (File S1). Although the frequency of illegitimate mating is slightly reduced in *sae2*Δ mutants, classes 3A and 3C remain the largest category of illegitimate diploids, indicating that repair of FS2-associated DSBs by BIR is independent of Sae2p.

Most chromosome rearrangements requiring BIR-mediated repair of a DSB at FS2 or FS1 are dependent on Rad52p: We monitored the frequencies of various classes of illegitimate diploids generated by mating *GAL-POL1* strains to a *rad52*Δ tester and by mating *GAL-POL1 rad52*Δ strains to a *rad52*Δ tester (Table 1). The frequencies of class 1 and class 2 diploids were not substantially affected by the *rad52*Δ mutation (Table 1). This result is expected since the formation of these classes does not require homologous recombination. In contrast, the frequency of class 3 events was reduced ~100-fold in the diploids formed by mating *GAL-POL1 rad52*Δ strains to a *rad52*Δ tester. Since most class 3 events reflect BIR (class 3A) or repair by recombination with the homolog (class 3B), events that require Rad52p (Symington 2002; Davis and Symington 2004), this result is also not surprising.

CHEF gel separation of chromosomes, Southern blotting, and microarrays were used to analyze 12 class 3 illegitimate diploids from *rad52*Δ strains. Five of these illegitimate diploids contained unusual rearrangements in which the repair product is consistent with single-strand annealing between the broken chromosome III and another broken chromosome, resulting in a "half-crossover" translocation (Haber and Hearn 1985; Smith *et al.* 2009). File S1 and Figure S2 contain a detailed discussion of the repair events in these illegitimate diploids. We also found two illegitimate diploids that contained deletions that appeared to reflect a DSB near FS2, followed by telomere addition. We used PCR to amplify the deletion breakpoint and determined the exact location of telomere additions in these two strains. Both breakpoints were located within the centromere-proximal Ty1 of FS2 near the spacer that separates the inverted pair of Ty elements (File S1 and Figure S3).

DISCUSSION

As described in the Introduction, palindromic sequences are associated with genetic instability in bacteria, yeast, and mammalian cells. We previously described a naturally occurring fragile site (FS2) composed of an inverted pair of Ty elements separated by a 280-bp spacer (Lemoine *et al.* 2005, 2008). In the current study, we contrast the regulation of genetic instability of FS2 from that reported for perfect palindromes or IRs with short spacers.

Formation of cruciform and hairpin secondary structures: Palindromes and IRs have been proposed to form two types of structures, cruciforms (Figure 1, left) and hairpins (Figure 1, right). Physical evidence for the existence of cruciforms has been obtained from *in vitro* and *in vivo* studies of plasmids and phage carrying perfect palindromes or IRs separated by <10 bp, but not from plasmids carrying IRs separated by ≥20 bp (Sinden *et al.* 1983, 1991; Zheng *et al.* 1991; Allers and Leach 1995; Kogo *et al.* 2007). However, IRs with large spacers can form hairpins on single-stranded DNA (Figure 1, right), such as within the Okazaki fragment initiation zone on the lagging strand during DNA replication (Trinh and Sinden 1991; Voineagu *et al.* 2008). The long central spacer at FS2 makes it likely that the recombinogenic structure formed by this sequence is a hairpin. In addition, the elevated rate of instability of spaced IRs (including FS2) under conditions of perturbed DNA replication is more consistent with hairpin formation than with cruciform formation (Gordenin *et al.* 1992; Lemoine *et al.* 2005, 2008). It should be noted that hairpin formation, rather than cruciform formation, has also been observed in *E. coli* for a 111-bp IR interrupted by a 24-bp central spacer (Eykelenboom *et al.* 2008).

DSB formation and homologous recombination at cruciform and hairpin structures: Cleavage of a cruciform by a Holliday junction resolvase would be predicted to yield two broken molecules with hairpin-capped ends (Figure 1A). In certain mutant yeast strains, Cote and Lewis (2008) reported such products in plasmids containing perfect palindromes, and Lobachev *et al.* (2002) observed these products at an IR consisting of a pair of inverted Alu elements separated by 12 bp. Thus, it has been proposed that there are two steps involved in the processing of cruciforms (Lobachev *et al.* 2002; Cote and Lewis 2008): (1) cleavage by a Holliday junction-like resolvase resulting in two hairpin-capped DSBs and (2) cleavage of the hairpin tips to generate a free 3′ end for repair by homologous recombination (Figure 1A).

Cote and Lewis (2008) reported that the first step, DSB formation, was independent of Mre11p and Sae2p but dependent on Mus81p. Mus81p acting with Mms4p has the ability to cleave certain types of branched DNA structures, although its activity *in vitro* is different from

that of a classic resolvase (reviewed by Mimitou and Symington 2009). In contrast to the results of the Lewis lab, DSB formation at the Alu-IR was independent of Mus81p, Mre11p, Sae2p, and also Yen1p (Lobachev *et al.* 2002; K. Lobachev, personal communication). Yen1p has the *in vitro* enzymatic activity expected for a Holliday junction resolvase (Ip *et al.* 2008). In agreement with the Lobachev lab, we found that DSB formation at FS2 is independent of all tested nucleases including Mre11p, Sae2p, Rad1p, Slx4p, Pso2p, Exo1p, Mus81p, Rad27p, and Yen1p. Thus, either the DSBs at FS2 are generated by an as-yet untested nuclease or these enzymes might act on the FS2-associated secondary structure in a functionally redundant manner.

Both Lobachev *et al.* (2002) and Cote and Lewis (2008) report that the second step of cruciform processing, cleavage of the hairpin tips to facilitate homologous recombination, is dependent on Sae2p and Mre11p. These results are consistent with other *in vivo* and *in vitro* studies (Rattray *et al.* 2001; Trujillo and Sung 2001; Farah *et al.* 2002; Lengsfeld *et al.* 2007). In *mre11*Δ and *sae2*Δ mutants, the hairpin tips persist and subsequent replication across the tip results in the formation of an extended inverted duplication centered at the site of the original palindrome or IR (Narayanan *et al.* 2006; Cote and Lewis 2008). A dicentric chromosome formed by this process could lead to chromosome rearrangements such as that shown in Figure 6. In yeast strains with a palindrome with a short spacer, such rearrangements are common (Narayanan *et al.* 2006). However, in the current study, we found only a single example of this type of repair product from *mre11* or *sae2* nuclease mutants. These results indicate that the two-step pathway of DSB formation and processing described for perfect palindromes and IRs with small spacers is unlikely to be the major pathway of DSB formation at FS2.

A hairpin structure at FS2 could be processed by endonucleases that cleave at the base of the hairpin (Figure 1, B and D) or by an endonuclease that cleaves the 280-bp single-stranded loop at the hairpin tip (Figure 1C). Processing by endonucleases as shown in Figure 1B is inconsistent with the observation that most of the chromosome rearrangements have a breakpoint in the centromere-proximal Ty of FS2. Processing of the FS2-associated hairpin as shown in Figure 1D followed by replication through the hairpin following cleavage would generate a centromere-containing chromosome with a DSB near the centromere-distal Ty of FS2. This Ty has not been observed at the breakpoint of rearrangements in our studies. We suggest that FS2-associated DSBs are generated by a single-step pathway as shown in Figure 1C, independent of Mre11p and Sae2p. This process would result in a centromere-containing broken chromosome with the centromere-proximal Ty element of FS2 at the end. Consistent with this model, most of the chromosome rearrangements that we mapped have this Ty element at the breakpoint, and the two terminal deletions that we analyzed were within this Ty element.

Chromosome rearrangements associated with the DSB at FS2: In this study, as in previous studies (Lemoine *et al.* 2005, 2008), the most common class of chromosome rearrangements was translocations reflecting BIR events in which the Ty elements of FS1 or FS2 recombined with a Ty or a δ-element on a nonhomologous chromosome. For the Ty elements on the broken chromosome to pair with nonallelic Ty elements, the broken end needs to be processed by nucleases that degrade the duplex 5′–3′, exposing the 3′ end required to initiate the exchange. In *S. cerevisiae*, this processing is carried out in two steps (Mimitou and Symington 2009), with one step leading to very short single-stranded "tails" (carried out by Sae2p and the MRX complex) and a second reaction leading to longer (several hundred bases) single-stranded ends carried out by Exo1p, Sgs1p complexed with Dna2p, or (possibly) Sgs1p complexed with Exo1p (Mimitou and Symington 2009). Loss of Sae2p or the MRX complex delays, but does not prevent, resection (Mimitou and Symington 2009), consistent with our finding that chromosome rearrangements were not prevented by mutations of *MRE11* or *SAE2*.

Some Ty elements appear to interact more frequently than others in generating translocations, although with the small number of events examined, these biases are not statistically significant. There are 31 Ty1 and Ty2 elements that are in the correct orientation to produce a monocentric translocation in a BIR event involving the centromere-proximal Ty element of FS2. Of 20 translocations involving this Ty element of FS2, 3 interacted with Ty1-1 on chromosome V and 3 interacted with Ty1-2 on IV. Interestingly, the Ty1-1 element on V was shown to be a hotspot for gamma ray-induced translocations (Argueso *et al.* 2008). There are 21 Ty1 and Ty2 elements in the correct orientation to produce a monocentric translocation by a BIR event with the FS1 Ty elements. Of 14 translocations examined, 3 involved Ty1-2 on chromosome II, and 4 involved a tandem pair of Ty elements (Ty1-1 and Ty1-2) on chromosome IV. If additional data support the preferential use of certain Ty elements in interacting with the FS1 and FS2 Ty's, there are a number of explanations: (1) certain elements have a more open chromatin configuration and are more susceptible to strand invasion, (2) the arrangement of chromosomes within the nucleus affects the frequency of interaction, and (3) the sequences of the Ty elements that interact frequently with the Ty elements of FS1 and FS2 are more similar than those elements that do not interact frequently. Unfortunately, since our genetic background is not identical to that of the sequenced yeast strains, investigation of the last possibility would require extensive resequencing.

Rad52p-independent chromosome rearrangements: half crossovers: Since the frequency of BIR events is

greatly reduced in *rad52*Δ strains (reviewed by Paques and Haber 1999; Llorente *et al.* 2008), the low frequency of class 3 events was expected. As described above, the most common type of rearrangement observed in the *rad52*Δ diploids was likely the result of a half crossover, the production of a single recombinant from two broken chromosomes (Haber and Hearn 1985). Since Ty or δ-elements were observed at the breakpoints of these chromosome rearrangements, it is likely that the recombinant chromosome was formed by single-strand annealing (SSA) between nonallelic Ty or δ-elements (Figure S2). Although the *rad52*Δ mutation reduces the frequency of SSA for small repeats, the effect on recombination between repeats >2 kb is minor (Paques and Haber 1999). For example, the rate of recombination in the tandem array of 9-kb rRNA gene repeats is unaffected by the *rad52*Δ mutation (Zamb and Petes 1981; Ozenberger and Roeder 1991).

Conclusion: On the basis of the data described above, we suggest that the processing of IRs with large spacers differs from the processing of perfect palindromes or IRs with short spacers. Perfect palindromes and IRs with short spacers can extrude as cruciforms and the processing of such structures to form recombinogenic DSBs is hypothesized to involve a two-step mechanism that is dependent on Mre11p and Sae2p (Rattray *et al.* 2001; Farah *et al.* 2002; Lobachev *et al.* 2002; Cote and Lewis 2008). In contrast, FS2 is an IR interrupted by a large spacer and likely does not extrude as a cruciform, but can form a hairpin on the lagging strand during replication. We propose that processing of the hairpin at FS2 to form a recombinogenic DSB occurs by a single-step mechanism that is independent of Mre11p and Sae2p. We suggest that the 280-base loop at the tip of the hairpin at FS2 is cleaved by a single-strand endonuclease; none of the nucleases examined in the current study (Mre11p, Sae2p, Rad1p, Slx4p, Pso2p, Exo1p, Mus81p, Yen1p, and Rad27p) are essential for this processing. The structure of the chromosome rearrangements associated with FS2-generated DSBs suggests that the broken chromosomes are repaired in a Rad52p-dependent BIR pathway involving nonallelic Ty elements.

We thank all members of the Petes lab for useful discussions and suggestions and Yiyong Liu for help in mapping chromosome deletion breakpoints. We thank M. Kupiec, K. Lobachev, and S. Jinks-Robertson for their comments on the manuscript. This study was supported by National Institutes of Health grant GM52319 to T.D.P.

LITERATURE CITED

Akgun, E., J. Zahn, S. Baumes, G. Brown, F. Liang *et al.*, 1997 Palindrome resolution and recombination in the mammalian germ line. Mol. Cell. Biol. **17:** 5559–5570.

Allers, T., and D. R. Leach, 1995 DNA palindromes adopt a methylation-resistant conformation that is consistent with DNA cruciform or hairpin formation in vivo. J. Mol. Biol. **252:** 70–85.

Argueso, J. L., J. Westmoreland, P. A. Mieczkowski, M. Gawel, T. D. Petes *et al.*, 2008 Double-strand breaks associated with repetitive DNA can reshape the genome. Proc. Natl. Acad. Sci. USA **105:** 11845–11850.

Bressan, D. A., H. A. Olivares, B. E. Nelms and J. H. Petrini, 1998 Alteration of N-terminal phosphoesterase signature motifs inactivates *Saccharomyces cerevisiae* Mre11. Genetics **150:** 591–600.

Collick, A., J. Drew, J. Penberth, P. Bois, J. Luckett *et al.*, 1996 Instability of long inverted repeats within mouse transgenes. EMBO J. **15:** 1163–1171.

Collins, J., G. Volckaert and P. Nevers, 1982 Precise and nearly-precise excision of the symmetrical inverted repeats of Tn5; common features of recA-independent deletion events in *Escherichia coli*. Gene **19:** 139–146.

Cote, A. G., and S. M. Lewis, 2008 Mus81-dependent double-strand DNA breaks at in vivo-generated cruciform structures in *S. cerevisiae*. Mol. Cell **31:** 800–812.

Courey, A. J., and J. C. Wang, 1988 Influence of DNA sequence and supercoiling on the process of cruciform formation. J. Mol. Biol. **202:** 35–43.

D'Amours, D., and S. P. Jackson, 2002 The Mre11 complex: at the crossroads of DNA repair and checkpoint signalling. Nat. Rev. Mol. Cell. Biol. **3:** 317–327.

DasGupta, U., K. Weston-Hafer and D. E. Berg, 1987 Local DNA sequence control of deletion formation in *Escherichia coli* plasmid pBR322. Genetics **115:** 41–49.

Davis, A. P., and L. S. Symington, 2004 *RAD51*-dependent break-induced replication in yeast. Mol. Cell. Biol. **24:** 2344–2351.

DePamphilis, M. L., 2002 Eukaryotic DNA replication forks. Chemtracts. Biochem. Mol. Biol. **15:** 313–325.

DePamphilis, M. L., and P. M. Wassarman, 1980 Replication of eukaryotic chromosomes: a close-up of the replication fork. Annu. Rev. Biochem. **49:** 627–666.

Edgar, R., M. Domrachev and A. E. Lash, 2002 Gene Expression Omnibus: NCBI gene expression and hybridization array data repository. Nucleic Acids Res. **30:** 207–210.

Eykelenboom, J. K., J. K. Blackwood, E. Okely and D. R. Leach, 2008 SbcCD causes a double-strand break at a DNA palindrome in the *Escherichia coli* chromosome. Mol. Cell **29:** 644–651.

Farah, J. A., E. Hartsuiker, K. Mizuno, K. Ohta and G. R. Smith, 2002 A 160-bp palindrome is a Rad50.Rad32-dependent mitotic recombination hotspot in *Schizosaccharomyces pombe*. Genetics **161:** 461–468.

Farah, J. A., G. Cromie, W. W. Steiner and G. R. Smith, 2005 A novel recombination pathway initiated by the Mre11/Rad50/Nbs1 complex eliminates palindromes during meiosis in *Schizosaccharomyces pombe*. Genetics **169:** 1261–1274.

Friedberg, E. C., G. C. Walker, W. Siede, R. D. Wood, R. A. Schultz *et al.*, 2006 *DNA Repair and Mutagenesis*. ASM Press, Washington, DC.

Gordenin, D. A., A. L. Malkova, A. Peterzen, V. N. Kulikov, Y. I. Pavlov *et al.*, 1992 Transposon Tn5 excision in yeast: influence of DNA polymerases α, δ, and ε and DNA repair genes. Proc. Natl. Acad. Sci. USA **89:** 3785–3789.

Gordenin, D. A., K. S. Lobachev, N. P. Degtyareva, A. L. Malkova, E. Perkins *et al.*, 1993 Inverted DNA repeats: a source of eukaryotic genomic instability. Mol. Cell. Biol. **13:** 5315–5322.

Guthrie, C., and G. R. Fink, 1991 *Guide to Yeast Genetics and Molecular Biology*. Academic Press, San Diego.

Haber, J. E., and M. Hearn, 1985 *RAD52*-independent mitotic gene conversion in *Saccharomyces cerevisiae* frequently results in chromosomal loss. Genetics **111:** 7–22.

Hawthorne, D. C., 1963 A deletion in yeast and its bearing on the structure of the mating type locus. Genetics **48:** 1727–1729.

Ip, S. C., U. Rass, M. G. Blanco, H. R. Flynn, J. M. Skehel *et al.*, 2008 Identification of Holliday junction resolvases from humans and yeast. Nature **456:** 357–361.

Kogo, H., H. Inagaki, T. Ohye, T. Kato, B. S. Emanuel *et al.*, 2007 Cruciform extrusion propensity of human translocation-mediating palindromic AT-rich repeats. Nucleic Acids Res. **35:** 1198–1208.

Kokoska, R. J., L. Stefanovic, J. DeMai and T. D. Petes, 2000 Increased rates of genomic deletions generated by muta-

tions in the yeast gene encoding DNA polymerase delta or by decreases in the cellular levels of DNA polymerase delta. Mol. Cell. Biol. **20:** 7490–7504.

Krishna, S., B. M. Wagener, H. P. Liu, Y. C. Lo, R. Sterk *et al.*, 2007 Mre11 and Ku regulation of double-strand break repair by gene conversion and break-induced replication. DNA Repair (Amst.) **6:** 797–808.

Kurahashi, H., H. Inagaki, T. Ohye, H. Kogo, T. Kato *et al.*, 2006 Palindrome-mediated chromosomal translocations in humans. DNA Repair (Amst.) **5:** 1136–1145.

Kurahashi, H., H. Inagaki, E. Hosoba, T. Kato, T. Ohye *et al.*, 2007 Molecular cloning of a translocation breakpoint hotspot in 22q11. Genome Res. **17:** 461–469.

Lemoine, F. J., N. P. Degtyareva, K. Lobachev and T. D. Petes, 2005 Chromosomal translocations in yeast induced by low levels of DNA polymerase a model for chromosome fragile sites. Cell **120:** 587–598.

Lemoine, F. J., N. P. Degtyareva, R. J. Kokoska and T. D. Petes, 2008 Reduced levels of DNA polymerase delta induce chromosome fragile site instability in yeast. Mol. Cell. Biol. **28:** 5359–5368.

Lengsfeld, B. M., A. J. Rattray, V. Bhaskara, R. Ghirlando and T. T. Paull, 2007 Sae2 is an endonuclease that processes hairpin DNA cooperatively with the Mre11/Rad50/Xrs2 complex. Mol. Cell **28:** 638–651.

Lewis, S. M., and A. G. Cote, 2006 Palindromes and genomic stress fractures: bracing and repairing the damage. DNA Repair (Amst.) **5:** 1146–1160.

Llorente, B., C. E. Smith and L. S. Symington, 2008 Break-induced replication: What is it and what is it for? Cell Cycle **7:** 859–864.

Lobachev, K. S., D. A. Gordenin and M. A. Resnick, 2002 The Mre11 complex is required for repair of hairpin-capped double-strand breaks and prevention of chromosome rearrangements. Cell **108:** 183–193.

Mimitou, E. P., and L. S. Symington, 2009 Nucleases and helicases take center stage in homologous recombination. Trends Biochem. Sci. **34:** 264–272.

Moreau, S., J. R. Ferguson and L. S. Symington, 1999 The nuclease activity of Mre11 is required for meiosis but not for mating type switching, end joining, or telomere maintenance. Mol. Cell. Biol. **19:** 556–566.

Narayanan, V., P. A. Mieczkowski, H. M. Kim, T. D. Petes and K. S. Lobachev, 2006 The pattern of gene amplification is determined by the chromosomal location of hairpin-capped breaks. Cell **125:** 1283–1296.

Ozenberger, B. A., and G. S. Roeder, 1991 A unique pathway of double-strand break repair operates in tandemly repeated genes. Mol. Cell. Biol. **11:** 1222–1231.

Paques, F., and J. E. Haber, 1999 Multiple pathways of recombination induced by double-strand breaks in *Saccharomyces cerevisiae*. Microbiol. Mol. Biol. Rev. **63:** 349–404.

Rattray, A. J., 2004 A method for cloning and sequencing long palindromic DNA junctions. Nucleic Acids Res. **32:** e155.

Rattray, A. J., C. B. McGill, B. K. Shafer and J. N. Strathern, 2001 Fidelity of mitotic, double-strand-break repair in *Saccharomyces cerevisiae*: a role for *SAE2/COM1*. Genetics **158:** 109–122.

Rattray, A. J., B. K. Shafer, B. Neelam and J. N. Strathern, 2005 A mechanism of palindromic gene amplification in *Saccharomyces cerevisiae*. Genes Dev. **19:** 1390–1399.

Rouse, J., 2009 Control of genome stability by Slx protein complexes. Biochem. Soc. Trans. **37:** 495–510.

Ruskin, B., and G. R. Fink, 1993 Mutations in POL1 increase the mitotic instability of tandem inverted repeats in *Saccharomyces cerevisiae*. Genetics **134:** 43–56.

Schmidt, K. H., V. Pennaneach, C. P. Putnam and R. D. Kolodner, 2006 Analysis of gross-chromosomal rearrangements in *Saccharomyces cerevisiae*. Methods Enzymol. **409:** 462–476.

Sinden, R. R., S. S. Broyles and D. E. Pettijohn, 1983 Perfect palindromic lac operator DNA sequence exists as a stable cruciform structure in supercoiled DNA in vitro but not in vivo. Proc. Natl. Acad. Sci. USA **80:** 1797–1801.

Sinden, R. R., G. X. Zheng, R. G. Brankamp and K. N. Allen, 1991 On the deletion of inverted repeated DNA in *Escherichia coli*: effects of length, thermal stability, and cruciform formation in vivo. Genetics **129:** 991–1005.

Smith, C. E., A. F. Lam and L. S. Symington, 2009 Aberrant double-strand break repair resulting in half crossovers in mutants defective for Rad51 or the DNA polymerase delta complex. Mol. Cell. Biol. **29:** 1432–1441.

Strathern, J., J. Hicks and I. Herskowitz, 1981 Control of cell type in yeast by the mating type. The alpha1-alpha2 hypothesis. J. Mol. Biol. **147:** 239–244.

Symington, L. S., 2002 Role of *RAD52* epistasis group genes in homologous recombination and double-strand break repair. Microbiol. Mol. Biol. Rev. **66:** 630–670.

Tanaka, H., D. A. Bergstrom, M. C. Yao and S. J. Tapscott, 2005 Widespread and nonrandom distribution of DNA palindromes in cancer cells provides a structural platform for subsequent gene amplification. Nat. Genet. **37:** 320–327.

Tanaka, H., Y. Cao, D. A. Bergstrom, C. Kooperberg, S. J. Tapscott *et al.*, 2007 Intrastrand annealing leads to the formation of a large DNA palindrome and determines the boundaries of genomic amplification in human cancer. Mol. Cell. Biol. **27:** 1993–2002.

Tavassoli, M., M. Shayeghi, A. Nasim and F. Z. Watts, 1995 Cloning and characterisation of the *Schizosaccharomyces pombe rad32* gene: a gene required for repair of double strand breaks and recombination. Nucleic Acids Res. **23:** 383–388.

Trinh, T. Q., and R. R. Sinden, 1991 Preferential DNA secondary structure mutagenesis in the lagging strand of replication in *E. coli*. Nature **352:** 544–547.

Trujillo, K. M., and P. Sung, 2001 DNA structure-specific nuclease activities in the *Saccharomyces cerevisiae* Rad50*Mre11 complex. J. Biol. Chem. **276:** 35458–35464.

VanHulle, K., F. J. Lemoine, V. Narayanan, B. Downing, K. Hull *et al.*, 2007 Inverted DNA repeats channel repair of distant double-strand breaks into chromatid fusions and chromosomal rearrangements. Mol. Cell. Biol. **27:** 2601–2614.

Voineagu, I., V. Narayanan, K. S. Lobachev and S. M. Mirkin, 2008 Replication stalling at unstable inverted repeats: interplay between DNA hairpins and fork stabilizing proteins. Proc. Natl. Acad. Sci. USA **105:** 9936–9941.

Warmington, J. R., R. Anwar, C. S. Newlon, R. B. Waring, R. W. Davies *et al.*, 1986 A 'hot-spot' for Ty transposition on the left arm of yeast chromosome III. Nucleic Acids Res. **14:** 3475–3485.

Zamb, T. J., and T. D. Petes, 1981 Unequal sister-strand recombination within the yeast ribosomal DNA does not require the *RAD52* gene product. Curr. Genet. **3:** 125–132.

Zheng, G. X., and R. R. Sinden, 1988 Effect of base composition at the center of inverted repeated DNA sequences on cruciform transitions in DNA. J. Biol. Chem. **263:** 5356–5361.

Zheng, G. X., T. Kochel, R. W. Hoepfner, S. E. Timmons and R. R. Sinden, 1991 Torsionally tuned cruciform and Z-DNA probes for measuring unrestrained supercoiling at specific sites in DNA of living cells. J. Mol. Biol. **221:** 107–122.

Communicating editor: J. Sekelsky

GENETICS

Supporting Information
http://www.genetics.org/cgi/content/full/genetics.109.106385/DC1

Chromosome Aberrations Resulting From Double-Strand DNA Breaks at a Naturally Occurring Yeast Fragile Site Composed of Inverted Ty Elements Are Independent of Mre11p and Sae2p

Anne M. Casper, Patricia W. Greenwell, Wei Tang and Thomas D. Petes

DOI: 10.1534/genetics.109.106385

FILE S1

Supporting Text

Sequencing results from Class 1 (His$^+$ Thr$^+$) illegitimate diploids: Genomic DNA was harvested from the *GAL-POL1* haploid, the wild-type 1225 *MAT*α tester strain, and six His$^+$ Thr$^+$ illegitimate diploids (DAMC590 to DAMC595) resulting from a mating between these haploid strains. Overlapping sets of primers were used to amplify the *MAT* locus region (chromosome III , 19858 – 201589) in two segments (primer set 1, AMC194 and AMC178; primer set 2, AMC172 and AMC174). PCR products were purified and sequenced using primers located within these products (all primers are described in Table S2). Sequencing results indicated six polymorphisms in this region between the two parent haploids. These polymorphisms are (Watson strand, 1225/*GAL-POL1*): T/C at 200,373; G/C at 200,426; T/A at 200,602; A/G at 200,626; G/C at 200,655; A/C at 201,185. Of the six illegitimate diploids sequenced, five had both sequences derived from the parental haploids. Thus, these diploids appear to reflect rare fusions of *MAT*α haploids rather than point mutations inactivating the *MAT*α locus. One illegitimate diploid, DAMC593, was homozygous for all polymorphisms within the *MAT*α locus that were derived from the *GAL-POL1* haploid. Since CHEF gel analysis indicated that this illegitimate diploid contains two normal-sized chromosome IIIs, it is likely that the DAMC593 strain was the result of a DSB centromere-proximal to the *MAT* locus in the 1225 haploid that was repaired by BIR using the *GAL-POL1* chromosome III as a template.

Characterization of Class 3 chromosome rearrangements in illegitimate diploids from *rad52*Δ cells: We examined twelve Class 3 illegitimate *rad52*Δ/*rad52*Δ diploids using CHEF gels, Southern blotting, and microarrays. The most common event (5 of 12 strains) had a pattern not observed previously in which sequences were deleted from chromosome III and from a non-homologous chromosome (PG270, PG273, PG284, PG298, and PG300; Table 2). The breakpoints of these deletions had Ty or delta elements, and each strain had a rearranged chromosome of the size calculated by adding the non-deleted segments of the chromosome. These rearrangements are likely to represent "half crossovers", an event in which two broken chromosomes join to produce one recombinant product (HABER and HEARN 1985; SMITH *et al.* 2009). For example, in the illegitimate diploid PG273, which has deletions on chromosomes I and III (Supporting Fig. S2A), we suggest that a FS2-associated DSB was processed by exonucleases, rendering the Tys at FS1 single-stranded (Supporting Fig. S2B). One of these Ty elements annealed to a single-stranded delta element resulting from a break on chromosome I to yield the rearrangement. The size of the rearranged chromosome is that predicted from this model, and PCR analysis confirms the I-III fusion (Supporting Fig. S2C).

Several other Class 3 diploids had rearrangements also consistent with single-strand annealing (SSA; PAQUES and HABER 1999). PG270 had a deletion on III between *MAT* and *HMR*; a deletion of this type could reflect either SSA between *MAT* and *HMR* or unequal crossing-over between the two repeats. PG286 was monosomic for chromosome III with the *HIS4*

allele from one parent and the *thr4* allele from the other. Such a chromosome could be formed by SSA between a chromosome fragment derived from the *GAL-POL1* haploid containing the *HIS4* allele with a chromosome fragment derived from the tester haploid containing the *THR4* allele.

Two strains (PG282 and PG283) had rearranged chromosomes of the size and microarray pattern consistent with BIR events (Table 2). In PG282, the chromosome rearrangement indicated that a FS2-associated DSB was repaired by a BIR event involving a Ty2 element on chromosome II (Table 2). The rearranged chromosome in PG283 was consistent with an FS2-associated DSB that was repaired by a BIR event involving a Ty2 element located on the left arm of III. Previous studies (reviewed by PAQUES and HABER 1999; LLORENTE *et al.* 2008) showed that BIR events are greatly reduced in strains lacking Rad52p. It is possible that the two events simply represent rare Rad52p-independent BIR events. Alternatively, these chromosome rearrangements could also reflect SSA events. For example, in the *GAL-POL1* haploid that gave rise to PG282, both chromosome III and II may have been broken in G2. If one daughter cell received the broken centromere-containing fragment of III, the acentric fragment of II, and an intact copy of II then, following mating with the tester, an SSA event fusing the broken fragments of II and III would mimic the microarray pattern generated by a BIR event. In summary, nine of twelve of the Class 3 *rad52*Δ/*rad52*Δ strains are explicable as reflecting SSA events.

Lastly, three of the Class 3 strains had terminal deletions of chromosome III. In two of these strains (PG297 and PG300), the deletion was near FS2. In the third strain (PG272), the deletion was located about 20 kb centromere-distal to FS2.

Mapping the precise location of telomere additions in two Class 3B *rad52*Δ/*rad52*Δ illegitimate diploids: As noted above, we found two *rad52/rad52* illegitimate diploids (PG297 and PG301) that contained deletions of the left arm of III distal to FS2 and no other detectable alterations. We hypothesized that these deleted chromosomes reflected a DSB near FS2, followed by telomere addition. We mapped the breakpoint of these deletions using a modification of the methods employed by CHEN *et al.* (1998). We isolated genomic DNA from PG297 and PG301 and used this for a PCR reaction with a forward primer located within Ty1 and a reverse primer containing telomeric repeats. Sequence analysis of the resulting DNA fragments showed that the two breakpoints were within the centromere-proximal Ty of FS2, located about 60 bp apart (Supporting Fig. S3). Since the breakpoints in these two strains are not within the central spacer between the two inverted Ty1 elements of FS2, we suggest that a DSB occurring within the spacer of FS2 was processed before telomere addition. Since telomere capping of non-telomeric sequences is not random (PENNANEACH *et al.* 2006), processing of the break could facilitate exposure of a preferred site for telomere addition. We cannot, however, rule out the alternative possibility that the FS2-associated break occurs near, rather than within, the spacer.

CHEF, microarray, and Southern blot analysis of illegitimate diploids: Below, we describe the data that were used to diagnose the chromosome aberrations described in Table 1 of the main text. Most of the hybridization probes used in the analysis described below were generated by PCR amplification of genomic DNA using 20 base primers. The sequences within the PCR product are described using *Saccharomyces* Genome Database (SGD) coordinates.

DAMC144 resulted from a mating of PG238 x 1225α (relevant genotype *mre11-H125N/MRE11*). Genomic microarray analysis indicated a deletion on chromosome III distal to FS2, and duplication of chromosome II sequences distal to *YBLWTy2-1*. CHEF gel separation of chromosomes followed by Southern blotting using a *CHA1* probe to the left arm of chromosome III (chromosome III sequences 15838 – 16800) revealed a novel band at ~225 kb. This band also hybridized to the probe P2, which is immediately proximal to FS2 (chromosome III sequences 166957 – 167967) and to an *ECM21* probe located immediately distal to *YBLWTy2-1* (chromosome II sequences 27537 – 28182). The combined size of the chromosome III fragment (188 kb) and the chromosome II duplication (30 kb) is 218 kb, which agrees with the approximate size of the novel chromosome observed on the CHEF gel. These results are consistent with a III-II translocation generated by a BIR event between the centromere-proximal Ty1 element of FS2 and *YBLWTy2-1*.

DAMC145 resulted from a mating of PG238 x 1225 α (relevant genotype *mre11-H125N/MRE11*). Genomic microarray analysis indicated a deletion on chromosome III distal to FS1, and a duplication on chromosome X of distal to the tandem pair of Ty1 elements *YJRWTy1-1, YJRWTy1-2*. CHEF gel separation of chromosomes followed by Southern blotting using a *CHA1* probe showed a novel band at ~440 kb. This band also hybridized to the probe 17Cdown, which is immediately proximal to FS1 (chromosome III sequences 147248 – 147885), and to a *YJR030C* probe located immediately distal to *YJRWTy1-2* (chromosome X sequences 485018 – 485931). The combined size of the chromosome III fragment (150 kb) and the chromosome X duplication (273 kb) is 423 kb, approximately the size of the novel chromosome observed on the CHEF gel. These results are consistent with a III-X translocation generated by a BIR event between a Ty1 element of FS1 and *YJRWTy1-1* or *YJRWTy1-2*.

DAMC146 resulted from mating of PG238 x 1225 α (relevant genotype *mre11-H125N/MRE11*). Genomic microarray analysis indicated a deletion on chromosome III distal to FS2, and a duplication on chromosome VII distal to the inverted pair of Ty elements *YGRWTy2-2, YGRCTy1-3*. CHEF gel separation of chromosomes followed by Southern blotting using a *CHA1* probe revealed a novel chromosome at ~440 kb. This chromosome also hybridized to the P2 probe (described above). The combined size of the chromosome III fragment (188 kb) and the chromosome VII duplication (268 kb) is 456 kb, the approximate size of the novel chromosome observed on the CHEF gel. Further Southern analysis was done using an *Msc*I digest, and filters containing the restriction fragments were hybridized to the P2 probe and to the *TIF4631* probe located immediately distal to

YGRCTy1-3 (chromosome VII sequences 824064 – 824883). All results are consistent with a III-VII translocation generated by a BIR event between the centromere-proximal Ty1 element of FS2 and *YGRCTy1-3*.

DAMC215 resulted from mating of PG238 x 1225 α (relevant genotype *mre11-H125N/MRE11*). Genomic microarray analysis indicated a deletion on chromosome III distal to FS2, and a duplication on chromosome XVI distal to *YPLWTy1-1*. CHEF gel separation of chromosomes followed by Southern blotting using the *CHA1* probe revealed a novel chromosome of ~240 kb. This chromosome also hybridized to the P2 probe, and to an *APM1* probe located immediately distal to *YPLWTy1-1* (chromosome XVI sequences 51344 – 52223). The combined size of the chromosome III fragment (188 kb) and the chromosome XVI duplication (60 kb) is 248 kb, approximately the size of the novel chromosome observed on the CHEF gel. These results are consistent with a III-XVI translocation generated by a BIR event between the centromere-proximal Ty1 element of FS2 and *YPLWTy1-1*.

DAMC217 resulted from mating of PG238 x 1225 α (relevant genotype *mre11-H125N/MRE11*). Genomic microarray analysis indicated a deletion on III distal to FS1, and a duplication on chromosome X distal to *YJLCdelta4,5*. CHEF gel separation of chromosomes followed by Southern blotting using the *CHA1* probe showed a novel chromosome of ~500 kb. The combined size of the chromosome III fragment (150 kb) and the chromosome X duplication (355 kb) is 505 kb, the approximate size of the novel chromosome. Southern analysis was done using a *Bsa*HI digest, and filters containing the restriction fragments were hybridized to the probe 17Cdown (described above), and to the *YJL046down* probe (SGD coordinates 354025-354210). The *Bsa*HI fragment that hybridized to the *YJL046down* probe in MS71 was about 6 kb longer than predicted from the genomic sequence, suggesting the presence of an uncharacterized Ty insertion in this strain; GABRIEL *et al.* (2006) detected a Ty element at this position in the W303 strain. In summary, these results are consistent with a III-X translocation generated by a BIR event between the centromere-proximal Ty1 element of FS1 and a Ty or delta element on chromosome X.

DAMC220 was generated by mating of PG238 x 1225α (relevant genotype *mre11-H125N/MRE11*). Microarray analysis showed a deletion of sequences distal to FS2, and a duplication on IV of sequences distal to the inverted *Ty* pair *YDRWTy2-3, YDRCTy1-3*. CHEF gel analysis using the *CHA1* probe showed a novel chromosome of ~700 kb; this chromosome also hybridized to the P2 probe located centromere-proximal to FS2. The combined size of the chromosome III fragment (188 kb) and the chromosome IV duplication (540 kb) is 728 kb, the approximate size of the novel chromosome. These results are consistent with a III-IV translocation generated by a BIR event between the centromere-proximal Ty1 element of FS2 and *YDRCTy1-3*.

DAMC223 is the result of mating PG238 x 1225α (relevant genotype *mre11-H125N/MRE11*). The microarray analysis indicated a deletion on III distal to FS1, a duplication on chromosome XII of sequences between *YLRWTy1-2* and *YLR301W*, and a duplication on chromosome X distal to the tandem pair of *Ty1* elements *YJRWTy1-1, YJRWTy1-2*. CHEF gel analysis using the III-specific *CHA1* probe showed a novel chromosome of about ~630 kb. This chromosome was excised from the gel and subjected to microarray analysis. The band array revealed that the novel chromosome had III sequences from the left telomere to FS1 and chromosome XII sequences distal to *YLRWTy1-2*. The combined size of the chromosome III fragment (150 kb) and the chromosome XII fragment (479 kb) is 630 kb, the size of the novel chromosome observed on the CHEF gel. These results are consistent with a III-X translocation generated by a BIR event between a Ty1 element of FS1 and *YLRWTy1-2*. Since the genomic microarray detected an amplification on X and did not show amplification of the entire right arm of XII, this illegitimate diploid also contains additional chromosome rearrangements that we did not further characterize.

DAMC226 was generated by mating PG238 x 1225α (relevant genotype *mre11-H125N/MRE11*). Microarray analysis indicated a deletion of sequences distal to FS1 and a duplication on chromosome X distal to *YJLCdelta4,5*. Using the *CHA1* probe, we detected a novel chromosome of ~500 kb. The combined size of the chromosome III fragment (150 kb) and the chromosome X duplication (355 kb) is 505 kb, the size observed for the novel chromosome. These results are consistent with a III-X translocation generated by a BIR event between the centromere-proximal Ty1 element of FS1 and *YJLCdelta4,5* or the nearby Ty insertion (see analysis of DAMC217 above).

DAMC227 resulted from a cross of PG238 x 1225α (relevant genotype *mre11-H125N/MRE11*). Microarray analysis indicated a deletion distal to FS2 and duplication on V distal to *YERCTy1-2*. By CHEF gel analysis with a *CHA1* probe, we observed a novel chromosome of ~260 kb. This chromosome was excised from the gel and subjected to microarray analysis. The band array revealed that the novel chromosome had chromosome III sequences from the left telomere to FS2, and the right arm of V distal to *YERCTy1-2*. The combined size of the chromosome III (188 kb) and V fragments (79 kb) is 267 kb, in agreement with the size of the novel chromosome. These results are consistent with a III-V translocation generated by a BIR event between the centromere-proximal Ty1 element of FS2 and *YERCTy1-2*.

DAMC230 was constructed by mating PG238 x 1225α (relevant genotype *mre11-H125N/MRE11*). Microarray analysis indicated a deletion distal to FS1, and a duplication on chromosome I distal to *YARWdelta7*. CHEF gel analysis using the *CHA1* probe detected a novel chromosome of ~194 kb. The combined size of the chromosome III fragment (150 kb) and the chromosome I duplication (40 kb) is 190 kb, the same size as the novel chromosome. These results are consistent with a III-I translocation generated by a BIR event between a delta associated with the Ty1 elements of FS1 and *YARWdelta7*.

DAMC233 was formed by mating PG238 x 1225α (relevant genotype *mre11-H125N /MRE11*). Microarray analysis indicated loss of sequences distal to FS2 and duplication of sequences on II distal to *YBLWTy1-1*. We found a novel chromosome ~412 kb that hybridized to the *CHA1* and P2 probes. The combined size of the chromosome III fragment (188 kb) and the chromosome II duplication (221 kb) is 409 kb, the same size as the observed novel chromosome. These results indicate that III-II translocation was generated by a BIR event between a delta associated with the Ty1 elements of FS1 and *YBLWTy1-1*.

DAMC238 was a diploid formed by mating of PG238 x 1225α (relevant genotype *mre11-H125N /MRE11*). The microarray analysis showed a deletion distal to FS2 and a duplication distal to *tR(UCU)M1* on XIII. CHEF gel analysis showed a novel chromosome of ~388 kb that hybridized to both the *CHA1* and P2 probes. The combined size of the chromosome III fragment (188 kb) and the chromosome XIII duplication (176 kb) is 364 kb, approximately the size of the novel chromosome. Further Southern analysis was done using *Bsa*HI and *Msc*I digests, and filters containing the restriction fragments were hybridized to the probe P2 and to the *RNT1* probe located immediately distal to *tR(UCU)M1* (chromosome XIII sequences 748313 – 749262). The *RNT1* hybridization signal from an MS71 parental haploid was about 6 kb longer than predicted from the genomic sequence, suggesting the presence of an uncharacterized Ty insertion in this strain. PCR analysis using primers flanking the uncharacterized Ty insertion on XIII (primer AMC150 5'aaacaaagagctgccattcc3' and primer AMC152 5'tgtgctacatacaaaaccttc3') and primers in either the 5' end of Ty1 (5'gagttagccttagtggaagccttc3') or the 3' end of Ty1 (5'cgtatactacatcgagaccaagaag3') show the presence of a Ty insertion in the Crick orientation. A Ty insertion at this position was also observed in W303 (GABRIEL *et al.* 2006). The results suggest that the III-XIII translocation was generated by a BIR event between the centromere-proximal Ty1 element of FS2 and the Ty element immediately centromere-proximal to *RNT1* on XIII.

DAMC458 was formed by mating of AMC82 x 1225α (relevant genotype *mre11*Δ */MRE11*). Microarray analysis showed a deletion distal to FS1, and a duplication distal to *YARWTy1-1* on chromosome I. By CHEF gel analysis with the *CHA1* probe, we detected a novel chromosome of ~230 kb. The combined size of the chromosome III fragment (150 kb) and the chromosome II duplication (80 kb) is 230 kb, the size of the observed novel chromosome. Our analysis is consistent with a III-I translocation generated by a BIR event between a delta associated with the Ty1 elements of FS1 and *YARWTy1-1*.

DAMC461 results from mating of AMC82 x 1225α (relevant genotype *mre11*Δ */MRE11*). Microarray analysis showed a deletion distal to FS2, an interstitial duplication of VII between the inverted Ty pair *YGRWTy2-2*, *YGRCTy1-3* and ARS734, and trisomy of chromosome XII. Using the *CHA1* probe, we detected a novel chromosome of ~250 kb. The combined size of the

chromosome III fragment (188 kb) and the chromosome VII duplication (187 kb) is 375 kb, which does *not* agree with the size of the novel chromosome. Thus, this strain contains complex rearrangements that we did not characterize further.

DAMC464 was generated by mating of AMC82 x 1225α (relevant genotype *mre11*Δ */MRE11*). By microarray analysis, we showed a deletion of sequences distal to FS1, and a duplication distal to the tandem pair of Ty1 elements *YJRWTy1-1, YJRWTy1-2* on X. The size of the novel chromosome by CHEF gel analysis with the *CHA1* probe was ~440 kb. The combined size of the chromosome III fragment (150 kb) and the chromosome X duplication (273 kb) is 423 kb, in agreement with the size of the observed novel chromosome. We hypothesize that the III-X translocation was generated by a BIR event between a Ty1 element of FS1 and *YJRWTy1-1* or *YJRWTy1-2*.

DAMC467 resulted from mating of AMC82 x 1225α (relevant genotype *mre11*Δ */MRE11*). The microarray analysis indicated a deletion distal to FS2, and a duplication on chromosome V distal to *YERCTy1-1*. By CHEF analysis with the *CHA1* probe, we observed a novel chromosome of ~315 kb. The combined size of the chromosome III fragment (188 kb) and the chromosome V duplication (128 kb) is 316 kb, the size of the novel chromosome. These results are consistent with a III-V translocation generated by a BIR event between the centromere-proximal Ty1 element of FS2 and *YERCTy1-1*.

DAMC473 was constructed by mating PG238 x PG243 (relevant genotype *mre11-H125N / mre11-H125N*). By microarray analysis, we found a deletion of sequences distal to FS1, and a duplication distal to the tandem pair of Ty1 elements *YJRWTy1-1, YJRWTy1-2* on X. By CHEF gel analysis, there was a novel chromosome of about 436 kb that hybridized to the *CHA1*, the 17Cdown, and the *YJR030C* hybridization probes; the *YJR030C* probe is located immediately distal to *YJRWTy1-2* (chromosome X sequences 485018 – 485931). The combined size of the chromosome III fragment (150 kb) and the chromosome X duplication (273 kb) is 423 kb, approximately the size of the novel chromosome. These results are consistent with a III-X translocation generated by a BIR event between a Ty1 element of FS1 and *YJRWTy1-1* or *YJRWTy1-2*.

DAMC474 was generated by mating PG238 x PG243 (relevant genotype *mre11-H125N / mre11-H125N*). The microarray analysis showed a deletion distal to FS2, and a duplication on V of sequences distal to *YERCTy1-1*. The CHEF gel analysis (*CHA1* probe) revealed a novel chromosome of ~300 kb. The size is approximately that expected from the combined size of the chromosome III fragment (188 kb) and the chromosome V duplication (128 kb). Our results, therefore, suggest that the III-V translocation was generated by a BIR event between the centromere-proximal Ty1 element of FS2 and *YERCTy1-1*.

DAMC475 resulted from mating PG238 x PG243 (relevant genotype *mre11-H125N / mre11-H125N*). Microarray analysis showed a deletion distal to FS1, and a duplication on II distal to *YBRWTy1-2*. CHEF gel analysis (*CHA1* probe) indicated a novel chromosome of ~727 kb. The combined size of the chromosome III fragment (150 kb) and the chromosome II duplication (553 kb) is 703 kb, similar to that observed for the novel chromosome. Southern analysis was done using *Bsa*HI digest and *Nar*I/*Xba*I double digest, and filters containing the restriction fragments were hybridized to the probe 17Cdown (immediately proximal to FS1) and to the *YBR013C* probe (immediately distal to *YBRWTy1-2*, chromosome II sequences 265531 – 265859). These results suggest that the III-II translocation was generated by a BIR event between the centromere-proximal Ty1 element of FS1 and *YBRWTy1-2*.

DAMC476 resulted from a mating of PG238 x PG243 (relevant genotype *mre11-H125N / mre11-H125N*). The microarray analysis showed a deletion of sequences distal to FS2, a duplication of III sequences between FS1 and FS2, and a duplication on XIV distal to *YNLWTy1-2*. The CHEF gel analysis showed a novel chromosome of ~776 kb that hybridized to *CHA1*. Southern analysis was done using *Bsa*BI, *Bam*HI and *Avr*II digests and filters containing the restriction fragments were hybridized to the probe P2, which is immediately proximal to FS2. These digests confirmed that the amplification between FS1 and FS2 is in the form of an extended palindrome centered at FS2. The *Bam*HI digest was also hybridized to the *POR1* probe, which is immediately distal to *YNLWTy1-2* (chromosome XIV sequences 518149 – 518649). This analysis was consistent with a III-XIV translocation generated by a BIR event between the centromere-proximal Ty1 element of the inverted second copy of FS1 and *YNLWTy1-2*. The combined size of the chromosome III fragment (188 kb), the chromosome III duplication (54 kb) and the chromosome XIV duplication (525 kb) is 767 kb, in agreement with the size of the novel chromosome. The structure of this rearrangement and a mechanism that resulted in the rearrangement is shown in Figure 6. Similar rearrangements were observed by NARAYANAN *et al.* (2006).

DAMC479 was constructed by mating PG238 x PG243 (relevant genotype *mre11-H125N / mre11-H125N*). By microarray analysis, we found a deletion distal to FS1, and a duplication of sequences distal to *YARWdelta7* on I. CHEF gel analysis with the *CHA1* probe showed a novel chromosome of ~250 kb. The combined size of the chromosome III (150 kb) and I fragments (40 kb) is 190 kb. Although this size is significantly smaller than that observed for the novel chromosome, the two unrearranged copies of chromosome I in the parental haploids differ in size by about 30 kb, complicating the analysis. The orientations of the repetitive elements on I and III are consistent with the possibility of a BIR event between a delta associated with FS1 and *YARWdelta7*.

DAMC483 was formed by mating PG238 x PG243 (relevant genotype *mre11-H125N / mre11-H125N*). The microarray analysis showed a deletion of all sequences on III except those centromere-distal to *YCLWTy2-1* on the left arm (the left arm hot spot [LAHS] described by WARMINGTON *et al.* 1986). In addition, this strain had a deletion of the left arm of chromosome II of all sequences distal to *YBLWTy2-1*. The predicted size for a translocated chromosome containing the remaining fragments of III (90 kb) and II (784 kb) is 874 kb. CHEF gel analysis showed a novel chromosome of ~850 kb that hybridized to both the *CHA1* and *ATP1* probes; the latter probe is located immediately centromere-proximal to *YBLWTy2*-1 (37140 – 37779). These results are consistent with a III-II translocated chromosome resulting from repair by single-strand annealing of breaks at or near the repetitive elements involved.

DAMC484 was constructed by mating PG238 x PG243 (relevant genotype *mre11-H125N/ mre11-H125N*). Our microarray analysis showed a deletion distal to FS2, and a duplication distal to the inverted *Ty* pair *YDRCTy1-2*, *YDRWTy2-2* on IV. CHEF gel analysis with the *CHA1* probe showed a novel chromosome of ~813 kb. The combined size of the chromosome III fragment (188 kb) and the chromosome IV duplication (648 kb) is 836 kb, agreeing with the size of the novel chromosome. These results are consistent with a III-IV translocation produced by a BIR event between the centromere-proximal Ty1 element of FS2 and *YDRCTy1-2*.

DAMC485 was the product of the mating PG238 x PG243 (relevant genotype *mre11-H125N/ mre11-H125N*). By CHEF gel analysis using the *CHA1* probe, we identified a novel chromosome of about 194 kb. Microarray analysis demonstrated a deletion of sequences distal to FS2, but no other deletions or additions. These results indicate that the novel chromosome reflected a DSB at or near FS2 that was repaired by telomere capping.

DAMC495 was generated by mating PG238 x PG243 (relevant genotype *mre11-H125N/ mre11-H125N*). The microarray analysis showed a deletion distal to FS1, and a duplication of sequences distal to *YBLWTy2-1* on II. Using *CHA1* as a probe, we observed a novel chromosome of ~194 kb; this chromosome also hybridized to an *ECM21* probe located immediately distal to *YBLWTy2-1* (SGD coordinates 27537 – 28182). The combined size of the chromosome III fragment (150 kb) and the chromosome II duplication (29 kb) is 179 kb, approximately the size of the novel chromosome. Despite this agreement between the predicted and observed sizes of the chromosome alteration, the Ty elements involved are in the wrong orientation for a BIR event. It is possible that there is an undescribed additional Ty or delta element near *YBLWTy2-1*, although we have not proven this possibility.

DAMC536 was constructed by mating AMC189 x AMC195 (relevant genotype *sae2*Δ / *sae2*Δ). Microarray analysis indicated a deletion distal to FS2, and a duplication on V distal to *YERCTy1-1*. A novel chromosome of ~300 kb was observed using the *CHA1* probe. A band array of this chromosome showed that it contained the expected portions of III and V. The combined size of the III (188 kb) and the V fragments (128 kb) is 308 kb, close to the size of the novel chromosome. We conclude that the translocation was generated by a BIR event between the centromere-proximal Ty1 element of FS2 and *YERCTy1-1*.

DAMC539 was generated by mating AMC189 x AMC195 (relevant genotype *sae2*Δ / *sae2*Δ). The microarray analysis showed a deletion distal to FS2, and a duplication of II distal to *YBLCdelta7*. Using the *CHA1* probe, we observed a novel chromosome of ~400 kb. The size of this chromosome is consistent with that expected from the sizes of the chromosome III (188 kb) and II fragments (197 kb). There is a Watson-oriented Ty element immediately adjacent to *YBLCdelta7* in the parental MS71-derived experimental haploid that is not present in the SGD sequenced strain (ARGUESO *et al.* 2008). In conclusion, the III-II translocation was generated by a BIR event between the centromere-proximal Ty1 element of FS2 and the Watson-oriented Ty element adjacent to *YBLCdelta7*.

DAMC547 resulted from the mating of AMC189 x AMC195 (relevant genotype *sae2*Δ / *sae2*Δ). Microarray analysis indicated a deletion on III between the *MAT* locus and *HMR*. The predicted size for a chromosome with this deletion is 247 kb; this deletion has been observed previous by HAWTHORNE (1963). By CHEF gel analysis using *CHA1* as a hybridization probe, we found a novel chromosome of ~250 kb. This deletion could reflect either unequal crossing-over between *MAT* and *HMR* or an SSA event between these two repeats.

DAMC549 was a product of a cross of AMC189 x AMC195 (relevant genotype *sae2*Δ / *sae2*Δ). Microarray analysis showed a deletion distal to FS1, and a duplication on VII distal to *YGLWdelta3*. CHEF gel analysis (*CHA1* probe) revealed a novel chromosome of ~250 kb. This size is consistent with that expected from combining the III (150 kb) and VII (115 kb) fragments. Despite this concurrence, *YGLWdelta3* is in the wrong orientation to act as a template for BIR of a DSB at FS1 in production of a monocentric chromosome. Since we have detected a Crick Ty element near *YGLWdelta3* (not annotated in SGD), the III-VII translocation likely reflects a BIR event between one of the Ty elements in FS1 and the unannotated Ty element.

DAMC550 resulted from mating AMC189 x AMC195 (relevant genotype *sae2*Δ / *sae2*Δ). Microarray analysis indicated a deletion of sequences distal to FS2, a duplication on III between *YCRCdelta6* and FS1, and a duplication on X distal to the tandem pair of Ty1 elements *YJRWTy1-1, YJRWTy1-2*. The novel chromosome hybridizing to *CHA1* was ~440 kb. The combined size of the chromosome III fragment (188 kb), the chromosome III duplication (54 kb) and the chromosome X

duplication (273 kb) is 485 kb, close to the size of the novel chromosome. Southern blot analysis of *Bsp*EI restriction fragments hybridized to Probe 1 (chromosome III sequences 148247 – 148547; VANHULLE *et al.* 2007) confirmed that the duplication between *YCRCdelta6* and FS1 is an inverted repeat. The mechanism describing the nature of this rearrangement (similar to that proposed by VANHULLE *et al.* 2007) is shown in Supplemental Figure S1.

DAMC551 was constructed by crossing AMC82 x AMC198 (relevant genotype *mre11*Δ / *mre11*Δ). Microarray analysis showed a deletion distal to FS2, and a duplication of sequences on XII beginning in the rDNA and extending to the end of XII. The *CHA1* probe hybridized to a novel chromosome of ~2 Mb, which is consistent with the chromosome size expected for a III-XII translocated chromosome that includes the rDNA array. Although Ty insertions have been detected within the rDNA of some strains (VINCENT and PETES 1986), we have not looked for Ty insertions in the rDNA of our strains. Thus, although our data are consistent with the possibility of a BIR event between the centromere-proximal Ty element of FS2 and a Watson-oriented Ty element within the rDNA, this scenario has not yet been confirmed.

DAMC552 resulted from mating AMC82 x AMC198 (relevant genotype *mre11*Δ / *mre11*Δ). The microarray analysis indicated a deletion distal to FS2, and a duplication on II distal to *YBLCdelta7*. Using the *CHA1* probe, we observed a novel chromosome of ~388 kb. The combined size of the III fragment (188 kb) and the II duplication (197 kb) is 385 kb, about the same size as the novel chromosome. There is a Ty in the Watson orientation immediately adjacent to *YBLCdelta7* in the parental MS71-derived haploid that is not annotated in SGD (ARGUESO *et al.* 2008). These results suggest that the III-II translocation was generated by a BIR event between the centromere-proximal Ty1 element of FS2 and this unannotated Ty element.

DAMC553 was generated by mating AMC82 x AMC198 (relevant genotype *mre11*Δ / *mre11*Δ). Microarray analysis showed a deletion distal to FS1, and no other amplifications or deletions. With the *CHA1* probe, we observed a novel chromosome of ~242 kb. Since a telomere-capped deletion of III at FS1 would produce a chromosome of about 150 kb, the novel chromosome must contain additional chromosomal sequences. We did not analyze this rearrangement further.

DAMC555 was obtained by mating AMC82 x AMC198 (relevant genotype *mre11*Δ / *mre11*Δ). By microarray and CHEF gel analysis, this diploid was the result of a DSB near FS2 in which the broken end was capped by telomere addition, producing a novel chromosome of about 194 kb.

DAMC560 was produced by mating AMC82 x AMC198 (relevant genotype *mre11*Δ / *mre11*Δ). The microarray analysis indicated a deletion distal to FS2, and a duplication on XV distal to *YOLWTy1-1*. Using *CHA1* as a probe, we detected a novel

chromosome of ~300 kb. The combined size of the III fragment (188 kb) and the II duplication (124 kb) is 312 kb, in agreement with the size of the novel chromosome. The structure of the translocation junction was also confirmed by PCR (details in Fig. 5). These results are consistent with a III-XV translocation generated by a BIR event between the centromere-proximal Ty1 element of FS2 and *YOLWTy1-1*.

DAMC561 was generated by mating AMC82 x AMC198 (relevant genotype *mre11*Δ / *mre11*Δ). The microarray analysis showed a deletion distal to FS1, and a duplication on II distal to *YBRWTy1-2*. Using the *CHA1* probe, we observed a novel chromosome of ~700 kb. The combined size of the III fragment (150 kb) and the II duplication (553 kb) is 703 kb, approximately the size of the novel chromosome. Southern analysis was done using *Bsa*HI digest and *Nar*I/*Xba*I double digest and filters containing the restriction fragments were hybridized to the probe 17Cdown (described above), and to the *YBR013C* probe (distal to *YBRWTy1-2*, SGD coordinates 265531 – 265859). All results are consistent with a III-II translocation generated by a BIR event between the centromere-proximal Ty1 element of FS1 and *YBRWTy1-2*.

PG270 was constructed by mating PG250/PG251 x PG234 (relevant genotype *rad52*Δ / *rad52*Δ). The microarray analysis showed a deletion of all III except for the region on the left arm centromere-distal to *YCLWTy2-1* (the left arm hot spot, LAHS) (WARMINGTON *et al.* 1986); in addition, there was deletion on VII of all sequences distal to *YGRCTy1-2/YGRTy2-1*. The predicted size for a translocation containing the two remaining fragments of III and VII is 647 kb. Using the *KCC4* hybridization probe for the left arm of III (SGD coordinates 81455-81883), we detected a novel chromosome of ~654 kb; this chromosome also hybridized to an *ADE5,7* probe from the left arm of chromosome VII (SGD coordinates 56279-57553). DNA was digested using *Nsi*I and membranes containing the resulting restriction fragments were hybridized to an *ORM1* probe (SGD coordinates on VII, SGD 560823-561296). These results support the conclusion that the novel chromosome reflects a half crossover generated by SSA between *YCLWTy2-1* and one of the one of the *YGRCTy1-2/YGRTy2-1* pair of elements.

PG271 was constructed by mating PG250/PG251 x PG234 (relevant genotype *rad52*Δ / *rad52*Δ). The microarray analysis showed a deletion between the *MAT* locus and *HMR*, and no other changes. The predicted size for this deletion is 247 kb, and a novel chromosome of this size was observed by CHEF gel analysis with the *KCC4* hybridization probe. The result was also confirmed by band array analysis. This deletion is likely to be a consequence of SSA between *MAT* and *HMR*.

PG272 resulted from mating PG250/PG251 x PG234 (relevant genotype *rad52*Δ / *rad52*Δ). Microarray analysis indicated a terminal deletion of III initiating at *YGR034W*. The predicted size for a telomere-capped deletion at this site is about 216 kb, and we observed a novel chromosome about this size by CHEF gel analysis (*KCC4* probe). We performed a band array on the novel

chromosome and confirmed that no sequences derived from other yeast chromosomes were added to the truncated III. These results suggest that a DSB at or near *YGR034W* was repaired by telomere capping to generate the novel chromosome.

PG273 was constructed by mating PG250/PG251 x PG234 (relevant genotype *rad52*Δ / *rad52*Δ). The microarray analysis showed a deletion distal to FS1, and a deletion on chromosome I of the left arm, centromere, and right arm up to *YARWdelta6*. The predicted size for a translocated chromosome containing the two remaining fragments of III and I is 209 kb; this size was consistent with the observed novel chromosome (CHEF gel analysis using *KCC4* as a probe). These results suggest that the novel chromosome reflects a half crossover generated by SSA between one of the Ty elements of FS1 and *YARWdelta6*.

PG282 was constructed by mating PG250/PG251 x PG234 (relevant genotype *rad52*Δ / *rad52*Δ). The microarray analysis indicated a deletion on III of sequences distal to FS2, and a duplication of II distal to *YBLWTy2-1*. The predicted chromosome size for a translocation involving these two chromosomes at this breakpoint is about 220 kb. Using *KCC4* as a hybridization probe, we observed a novel chromosome of 218 kb. We did a band array of this chromosome and showed that it contained the expected III sequences plus sequences from the left arm of II (*YBLWTy2-1* to the left telomere). Thus, this chromosome could have been generated by a Rad52p-independent BIR event involving the centromere-proximal element of FS2 and *YBLWTy2-1*. Alternatively, as described in the text, the novel chromosome could reflect an SSA event.

PG283 resulted from mating PG250/PG251 x PG234 (relevant genotype *rad52*Δ / *rad52*Δ). Our microarray analysis showed a deletion distal to FS2, and an amplification of chromosome III sequences distal to *YCLWTy2-1*. This pattern could be explained by a break at or near FS2 that was repaired by a BIR event utilizing *YCLWTy2-1* as a template. The predicted size for this altered chromosome is 273 kb, close to the size (267 kb) observed by CHEF gel analysis with *KCC4* as the hybridization probe. As expected, band analysis revealed that sequences from the left telomere to *YCLWTy2-1* were present at twice the level of sequences from *YCLWTy2-1* to FS2, and all sequences distal to FS2 were deleted from the novel chromosome. In addition, genomic DNA was digested with *Bam*HI and a membrane containing the resulting restriction fragments was hybridized with probe P2, which is located centromere-proximal to FS2. The restriction map confirmed the nature of the rearrangement. In summary, the novel chromosome can be explained by a DSB at FS2 that was repaired by a BIR event involving *YCLWTy2-1*; alternatively, as with the chromosome rearrangement in PG282, an SSA event could generate the same chromosome alteration.

PG284 was constructed by mating PG250/PG251 x PG234 (relevant genotype *rad52*Δ / *rad52*Δ). The microarray indicated a deletion distal to FS2, and a deletion of all sequences on I except for those centromere distal to *YARCdelta8*. The predicted size for a translocation containing the two remaining fragments of III and I is 228 kb. The observed size of the novel chromosome

(CHEF gel analysis using *KCC4* as a probe) was ~230 kb. These results suggest that the novel chromosome reflects a half crossover generated by SSA between the centromere-proximal Ty of FS2 and *YARCdelta8*.

PG286 was generated by mating PG250/PG251 x PG234 (relevant genotype *rad52*Δ / *rad52*Δ). Our microarray analysis showed that this strain was monosomic for III, and had no other alterations. Since this strain was phenotypically $His^{+}Thr^{-}$, it was not generated by loss of a chromosome from either of the haploid parents. We suggest that this chromosome was formed by SSA between two broken copies of III in which the broken DNA molecule with a centromere was fused to a broken DNA molecular without a centromere to generate a single product. The left arm of this repaired chromosome III is from the *GAL-POL1 rad52*Δ haploid (since it contains the *HIS4* gene), and the right arm is from the *rad52*Δ tester strain (since it contains the *thr4* gene). An *Msc*I digest of genomic DNA, followed by Southern analysis of the restriction fragments with the P2 probe, was used to investigate the FS2 region of chromosome III. Since the *rad52*Δ tester haploid contains only one of the Ty1 elements of FS2, the *Msc*I fragments of the *GAL-POL1 rad52*Δ haploid and the *rad52*Δ tester strain differ in size by ~6 kb. PG286 had an *Msc*I fragment of the same size as the tester strain, indicating that the original breaks must have occurred at or centromere-proximal to FS2.

PG297 was created by mating PG250/PG251 x PG234 (relevant genotype *rad52*Δ / *rad52*Δ). The microarray analysis showed a deletion on chromosome III distal to FS2, and no other changes. The predicted size for a telomere-capped deletion at this site is 188 kb, and the observed size of a novel chromosome hybridizing to the *KCC4* probe was ~194 kb. Band analysis of this chromosome confirmed that it did not contain sequences from any other yeast chromosome. These results are consistent with a break at or near FS2 that was repaired by telomere capping. Using a PCR-based strategy, we mapped the precise breakpoint of the telomere addition (Fig. 8).

PG298 resulted from the mating PG250/PG251 x PG234 (relevant genotype *rad52*Δ / *rad52*Δ). The microarray analysis showed a deletion of III that removed everything except the sequences centromere-distal to *YCLWTy2-1*. In addition, there was a deletion of the left arm of chromosome VI distal to *YFLWTy2-1*. The predicted size for a translocation containing the two remaining fragments of III and VI is 217 kb; a novel chromosome of this size was detected by CHEF gel analysis (*KCC4* probe). The novel chromosome also hybridized to a *SPB4* probe centromere-proximal to *YFLWTy2*-1 on chromosome VI (SGD coordinates 145916-146843). DNA was digested using *Pst*I and membranes containing the resulting restriction fragments were hybridized to an *SPB1* probe and a *KCC4* probe. The restriction map demonstrated that PG298 ha a III-VI translocation consistent with its formation as a half crossover generated by SSA between *YCLWTy2-1* and *YFLWTy2-1*.

PG300 was generated by mating PG250/PG251 x PG234 (relevant genotype *rad52*Δ / *rad52*Δ). The microarray analysis showed a deletion distal to FS2, and a deletion of the left arm, centromere, and right arm of chromosome XII up to *YLRCdelta18*. The predicted size for a translocated chromosome containing the two remaining fragments of III and XII is 534 kb. CHEF gel analysis with the *KCC4* probe revealed a novel chromosome of ~557 kb. Thus, this chromosome is likely to reflect a half crossover generated by SSA between one of the FS2 Ty elements and *YLRCdelta18*.

PG301 was constructed by mating PG250/PG251 x PG234 (relevant genotype *rad52*Δ / *rad52*Δ). Microarray analysis showed a deletion on III of sequences distal to FS2. The predicted size for a telomere-capped deletion at this site is 188 kb. CHEF gel separation of chromosomes followed by Southern blotting using a *KCC4* probe to the left arm of chromosome III revealed a novel chromosome of ~194 kb. This band containing this chromosome was excised from the gel and subjected to microarray analysis. This array confirmed the deletion of sequences distal to FS2 and the absence of sequences from any other yeast chromosome. As described in Materials and Methods, using a PCR procedure, we demonstrated telomere capping of a DSB within the centromere-proximal Ty element of FS2.

REFERENCES

ARGUESO, J. L., J. WESTMORELAND, P. A. MIECZKOWSKI, M. GAWEL, T. D. PETES *et al.*, 2008 Double-strand breaks associated with repetitive DNA can reshape the genome. Proc Natl Acad Sci U S A **105:** 11845-11850.

CHEN, C., K. UMEZU and R. D. KOLODNER, 1998 Chromosome rearrangements occur in *S. cerevisiae* mutator mutants due to intergenic lesions processed by double-strand-break repair. Mol Cell **2:** 9-22.

GOLDSTEIN, A. L., and J. H. MCCUSKER, 1999 Three new dominant drug resistance cassettes for gene disruption in Saccharomyces cerevisiae. Yeast **15:** 1541-1553.

HABER, J. E. and M. HEARN, 1985 *RAD52*-independent mitotic gene conversion in *Saccharomyces cerevisiae* frequently results in chromosomal loss. Genetics **111:** 7-22.

HAWTHORNE, D. C., 1963 A Deletion In Yeast And Its Bearing On The Structure Of The Mating Type Locus. Genetics **48:** 1727-1729.

KOKOSKA, R. J., L. STEFANOVIC, J. DEMAI and T. D. PETES, 2000 Increased rates of genomic deletions generated by mutations in the yeast gene encoding DNA polymerase delta or by decreases in the cellular levels of DNA polymerase delta. Mol Cell Biol **20:** 7490-7504.

KOKOSKA, R. J., L. STEFANOVIC, H. T. TRAN, M. A. RESNICK, D. A. GORDENIN *et al.*, 1998 Destabilization of yeast micro- and minisatellite DNA sequences by mutations affecting a nuclease involved in Okazaki fragment processing (rad27) and DNA polymerase delta (pol3-t). Mol Cell Biol **18:** 2779-2788.

KROGH, B. O., B. LLORENTE, A. LAM and L. S. SYMINGTON, 2005 Mutations in Mre11 phosphoesterase motif I that impair Saccharomyces cerevisiae Mre11-Rad50-Xrs2 complex stability in addition to nuclease activity. Genetics **171:** 1561-1570.

LEMOINE, F. J., N. P. DEGTYAREVA, K. LOBACHEV and T. D. PETES, 2005 Chromosomal translocations in yeast induced by low levels of DNA polymerase a model for chromosome fragile sites. Cell **120:** 587-598.

LLORENTE, B., C. E. SMITH, and L. S. SYMINGTON, 2008 Break-induced replication: what is it and what is it for? Cell Cycle **7:** 859-864.

NARAYANAN, V., P. A. MIECZKOWSKI, H. M. KIM, T. D. PETES and K. S. LOBACHEV, 2006 The pattern of gene amplification is determined by the chromosomal location of hairpin-capped breaks. Cell **125:** 1283-1296.

PAQUES, F., and J. E. HABER, 1999 Multiple pathways of recombination induced by double-strand breaks in *Saccharomyces cerevisiae*. Microbiol Mol Biol Rev **63:** 349-404.

PENNANEACH, V., PUTNAM, C. D. and R. D. KOLODNER, 2006 Chromosome healing by *de novo* telomere addition in *Saccharomyces cerevisiae*. Mol Microbiol **59:** 1357-1368.

RITCHIE, K. B., J. C. MALLORY and T. D. PETES, 1999 Interactions of TLC1 (which encodes the RNA subunit of telomerase), TEL1, and MEC1 in regulating telomere length in the yeast Saccharomyces cerevisiae. Mol Cell Biol **19:** 6065-6075.

SMITH, C. E., A. F. LAM and L. S. SYMINGTON, 2009 Aberrant double-strand break repair resulting in half crossovers in mutants defective for Rad51 or the DNA polymerase delta complex. Mol Cell Biol **29:** 1432-1441.

VANHULLE, K., F. J. LEMOINE, V. NARAYANAN, B. DOWNING, K. HULL *et al.*, 2007 Inverted DNA repeats channel repair of distant double-strand breaks into chromatid fusions and chromosomal rearrangements. Mol Cell Biol **27:** 2601-2614.

VINCENT, A., and T. D. PETES, 1986 Isolation and characterization of a Ty element inserted into the ribosomal DNA of the yeast Saccharomyces cerevisiae. Nucleic Acids Res **14:** 2939-2949.

WARMINGTON, J. R., R. ANWAR, C. S. NEWLON, R. B. WARING, R. W. DAVIES *et al.*, 1986 A 'hot-spot' for Ty transposition on the left arm of yeast chromosome III. Nucleic Acids Res **14:** 3475-3485.

TABLE S1

Haploid strain genotypes and constructions

Strain name	Relevant genotype[a]	Reference or construction[c]
NPD1	*KANMX-GAL1-POL1*	(LEMOINE *et al.* 2005)
NPD44	*MATa KANMX-GAL1-POL1 can1 his1::HPH HIS7*	(LEMOINE *et al.* 2005)
FJL014	*KANMX-GAL1-POL1 FS2ΔCty::HYG*	(LEMOINE *et al.* 2005)
AMC3	*MATa KANMX-GAL1-POL1*	Spore colony from NPD1 x NPD44 cross
PG243[b]	*mre11-H125N*	Two-step transplacement of 1225α with the *URA3- mre11-H125N*-containing plasmid pSM438, linearized with *Sph*I (KROGH *et al.* 2005)
PG238	*KANMX-GAL1-POL1 mre11-H125N*	Two-step transplacement of NPD1 with the *URA3- mre11-H125N*-containing plasmid pSM438, linearized with *Sph*I (KROGH *et al.* 2005)
AMC198[b]	*mre11::HPH*	Transformation of 1225α with *mre11::HPH*; pAG32 template (GOLDSTEIN and MCCUSKER 1999); primers AMC073 (5'TGCTCCTCTCAAAATGGCATACCTTGTTGTTCG CGAAGGCAAGCCCTTGGcgtacgctgcaggtcgac) and AMC074 (5'GCAGACAATTGACGCAAGTTGTACCTGCTCAGA TCCGATAAAACTCGACTatcgatgaattcgagctc)
AMC56	*mre11::HPH*	Transformation of MS71 with *mre11::HPH*; pAG32 template (GOLDSTEIN and MCCUSKER 1999); primers AMC073 and AMC074 as above
AMC82	*KANMX-GAL1-POL1 mre11::HPH*	Spore colony from AMC56 x AMC3 cross
AMC195[b]	*sae2::HPH*	Transformation of 1225α with *sae2::HPH*; pAG32 template (GOLDSTEIN and MCCUSKER 1999); primers AMC113 (5'AATGTGTATCTAAAGTCAAGCTTATCCATTCTC AAGGAGCTCAGTCTCGAcgtacgctgcaggtcgac) and AMC114 (5'CTTTCTTCTGATGATTTCCTGGGATTTCTTTTT

		GTCCTCGTTCCCTTCCTatcgatgaattcgagctc)
AMC180	*sae2::HPH*	Transformation of MS71 with *sae2::HPH*; pAG32 template(GOLDSTEIN and MCCUSKER 1999); primers AMC113 and AMC114 as above
AMC189	*KANMX-GAL1-POL1 sae2::HPH*	Spore colony from AMC180 x AMC3 cross
RJK88	*MATa rad27*Δ	(KOKOSKA *et al.* 1998)
AMC50	*KANMX-GAL1-POL1 rad27*Δ	Spore colony from NPD1 x RJK88 cross
AMC54	*slx4::HPH*	Transformation of MS71 with *slx4::HPH*; pAG32 template (GOLDSTEIN and MCCUSKER 1999); primers AMC033 (5'CTATCTCTGTTCCATAATAATAACCAGTAGTTC AGTTGGGGAACTTAATAcgtacgctgcaggtcgac) and AMC034 (5'ATGACGGTATATATGCATATTTGTGTACGTGTA TTCTTCATCTATACGTAatcgatgaattcgagctc)
AMC76	*KANMX-GAL1-POL1 slx4::HPH*	Spore colony from AMC54 x AMC3 cross
AMC57	*rad1::HPH*	Transformation of MS71 with *rad1::HPH*; pAG32 template (GOLDSTEIN and MCCUSKER 1999); primers AMC050 (5'GAGAGAGCACAGGTGTACTGGAGGGTTCAGGA CGTTGGTAGAGCATTTGCcgtacgctgcaggtcgac) and AMC051 (5'AAGATTCAAAGAGCATGTCTAACTTATAACATA TACGGTCGAAGTCACCAatcgatgaattcgagctc)
AMC80	*KANMX-GAL1-POL1 rad1::HPH*	Spore colony from AMC57 x AMC3 cross
AMC59	*exo1::HPH*	Transformation of MS71 with *exo1::HPH*; pAG32 template (GOLDSTEIN and MCCUSKER 1999); primers AMC042 (5'TTTTCATTTGAAAAATATACCTCCGATATGAAAC GTGCAGTACTTAACTTcgtacgctgcaggtcgac) and AMC043 (5'ACCACATTAAAATAAAAGGAGCTCGAAAAAACT GAAAGGCGTAGAAAGGAatcgatgaattcgagctc)

AMC70	*KANMX-GAL1-POL1 exo1::HPH*	Spore colony from AMC59 x AMC3 cross
AMC60	*mus81::HPH*	Transformation of MS71 with *mus81::HPH*; pAG32 template (GOLDSTEIN and MCCUSKER 1999); primers AMC036 (5'AAACAAAGTTTCAAAGGATTGATACGAACACAC ATTCCTAGCATGAAAGCcgtacgctgcaggtcgac) and AMC037 (5'ATCACTTTTTTCTTTATAAAACCTTGCAGGGAT GACTATATTTCAAATTGatcgatgaattcgagctc)
AMC66	*KANMX-GAL1-POL1 mus81::HPH*	Spore colony from AMC60 x AMC3 cross
AMC67	*MAT*a *KANMX-GAL1-POL1 mus81::HPH*	Spore colony from AMC60 x AMC3 cross
AMC61	*pso2::HPH*	Transformation of MS71 with *pso2::HPH*; pAG32 template (GOLDSTEIN and MCCUSKER 1999); primers AMC039 (5'TACATTCATATAATATCCATTACGTACGTACATC TTACATAACACATTTTcgtacgctgcaggtcgac) and AMC40 (5'CATGTTAAGCAGCATACGCACTAGTGACTAATT TGGGTGGTCGGTTGATTatcgatgaattcgagctc)
AMC72	*KANMX-GAL1-POL1 pso2::HPH*	Spore colony from AMC61 x AMC3 cross
AMC202 [b]	*yen1::NAT*	Transformation of 1225α with *yen1::NAT*; pAG25 template (GOLDSTEIN and MCCUSKER 1999); primers AMC197 (5'AGTTCTATTGCATTTTACCTACTTGTATATTCT GGATACTGCACAAGAAAcgtacgctgcaggtcgac) and AMC198 (5'TCGGCGCGATCAACTGTGGTGGCGGATTTTTT GACGCTGTGCCCGTTAACatcgatgaattcgagctc)
AMC200 and AMC201	*yen1::NAT*	Transformation of MS71 with *yen1::NAT*; pAG25 template (GOLDSTEIN and MCCUSKER 1999); primers AMC197 and AMC198 as above
AMC217	*KANMX-GAL1-POL1 mus81::HPH yen1::NAT*	Spore colony from AMC67 x AMC201 cross
AMC204	*KANMX-GAL1-POL1 pso2::HPH*	Spore colony from AMC200 x AMC3 cross
PG234 [b]	*rad52::hisG-URA3-hisG*	Transformation of 1225α with *Bam*HI-treated pDTK102 (RITCHIE *et al.* 1999)

PG235	*rad52::hisG-URA3-hisG*	Transformation of MS71 with *Bam*HI-treated pDTK102 (RITCHIE *et al.* 1999)
PG250[d]	*KANMX-GAL1-POL1 rad52::hisG-URA3-hisG*	Spore colony from NPD44 x PG235 cross
PG251[d]	*KANMX-GAL1-POL1 rad52::hisG-URA3-hisG*	Spore colony from NPD44 x PG235 cross

[a] All strains (except those noted by superscript *b*) are isogenic with MS71, a *LEU2* derivative of AMY125 (α *ade5-1 leu2-3 trp1-289 ura3-52 his7-2*) (KOKOSKA *et al.* 2000) except for changes introduced by transformation as noted under "Relevant Genotype".

[b] All strains noted by superscript *b* are isogenic with 1225α (*MATα his4-15 leu2 thr4 ura3-52 trp1 lys*) except for changes introduced by transformation as noted under "Relevant Genotype".

[c] For strains constructed by transformation using PCR fragments to the targeted location, both the template for PCR amplification and primers are indicated. Primer sequences are shown with upper case letters corresponding to the targeted genomic regions and lower case letters corresponding to the selectable marker on the plasmid.

[d]PG250 and PG251 were different, but isogenic, haploids that gave similar results in illegitimate mating experiments.

TABLE S2

Primers used for sequencing the *MAT* locus in Class 1 (His$^+$ Thr$^+$) illegitimate diploids

Primer Name	Primer sequence (5' to 3')
AMC172	CCAGATTCCTGTTCCTTCCTC
AMC173	TCTTGCTCTTGTTCCCAATG
AMC173R	CATTGGGAACAAGAGCAAGACG
AMC174	TTGGAAACACCAAGGGAGAG
AMC178	TTTGACTTCCAGACGCTATC
AMC187	GCAATAAATTGCATCCCAAAC
AMC187R	GTTTGGGATGCAATTTATTGC
AMC188	TTGAAACCGCTGTGTTTCTG
AMC189	TCTTCAGCGAGCAGAGAAGAC
AMC194	ACTCTTCTTGAGACGATTTGG
AMC195	TTCGGGCTCATTCTTTCTTC
AMC196	TTTGTAAACCGGTGTCCTCTG
MATαF	GCACGGAATATGGGACTACTTCG
MATαR	CCACAAATCACAGATGAG

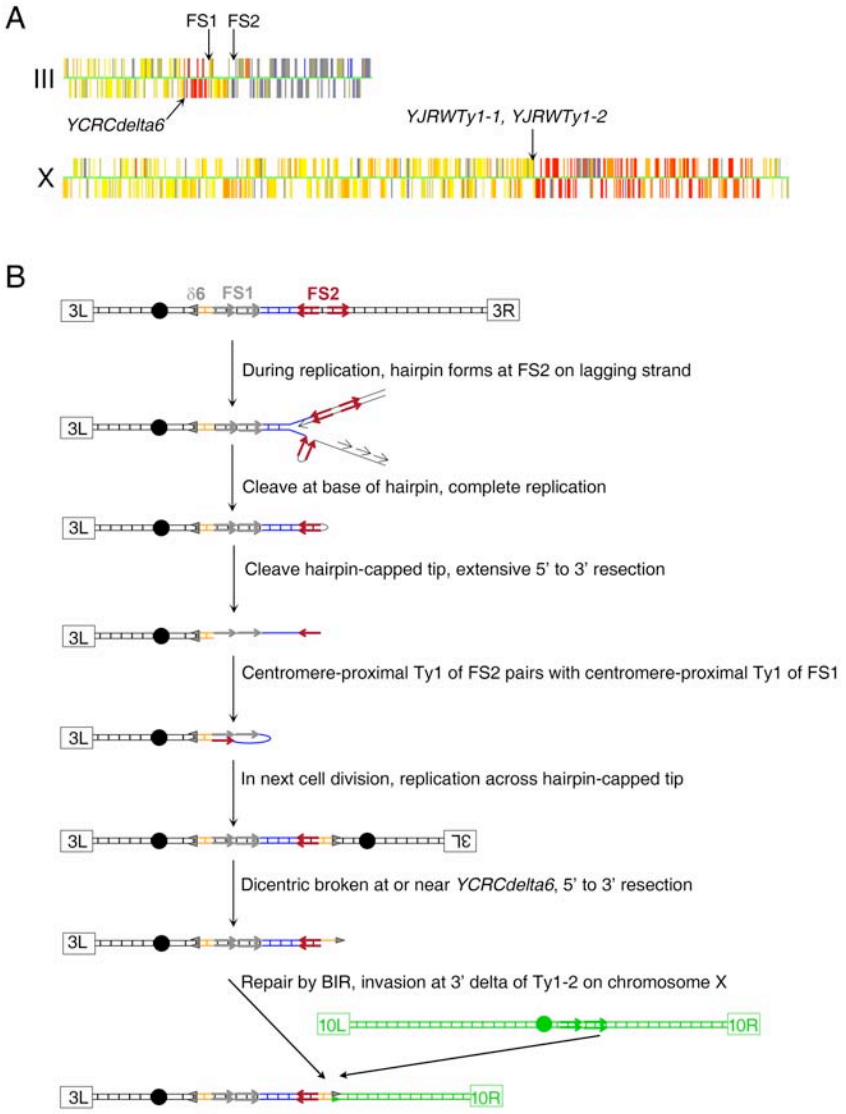

FIGURE S1.—Formation of a chromosome aberration as a consequence of interaction of Ty elements in FS2 and FS1 (illegitimate *sae2/sae2* diploid DAMC550). (A) Microarray analysis of DAMC550. In this depiction, the hybridization ratio for each ORF on the array is represented by a vertical line. Deletions and amplifications in the experimental strain relative to the control strain are shown in blue and red, respectively. No changes were observed except on chromosomes III and X. As shown, there is an amplification of III between *YCRCdelta6* and FS1, and a deletion of sequences distal to FS2. The amplification breakpoint on chromosome X is at the tandem pair of Ty elements *YJRWTy1-1*, *YJRWTy1-2*. (B) Mechanism for formation of the chromosome aberration in DAMC550; similar types of aberrations were detected by VANHULLE *et al.* (VANHULLE *et al.* 2007). Centromeres are indicated by black circles, left and right telomeres are identified by labeled rectangles, Ty elements are indicated by arrows, and *YCRCdelta6* is indicated by a gray arrowhead.

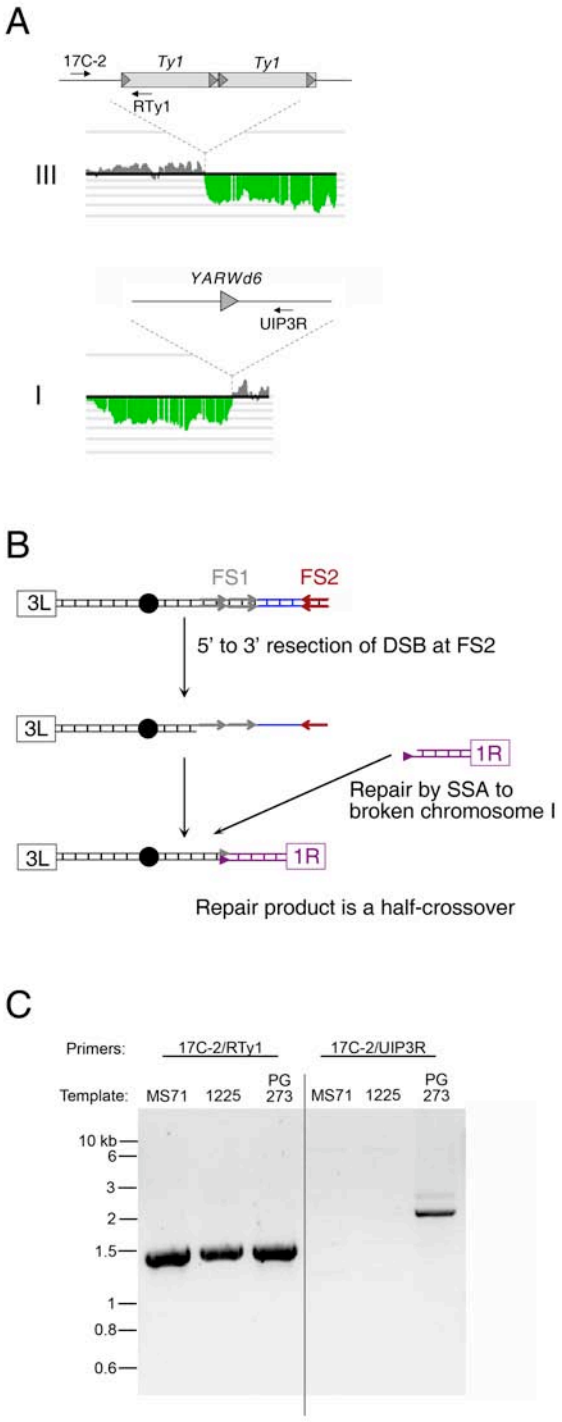

FIGURE S2.—Chromosome rearrangement resulting from a half crossover in the *rad52*Δ/*rad52*Δ illegitimate diploid PG273. (A) Microarray analysis. The illegitimate diploid PG273 had two deletions, one on chromosome III and one on I. The breakpoint on III was at FS1 and the breakpoint on I was at *YARWdelta6*. Ty elements, solo delta elements, and PCR primers are indicated by large gray arrows, gray arrowheads, and small black arrows, respectively. (B) Mechanism for producing a I-III translocation by SSA. Two broken chromosomes anneal by shared homology of non-allelic delta elements. (C) PCR analysis of the chromosome translocation in PG273. Primer locations are indicated in panel A of this figure. As expected, a PCR reaction using chromosome III (17C-2) and I (UIP3R) primers produces a product in PG273, but not in either the experimental (MS71) or tester (1225) strain.

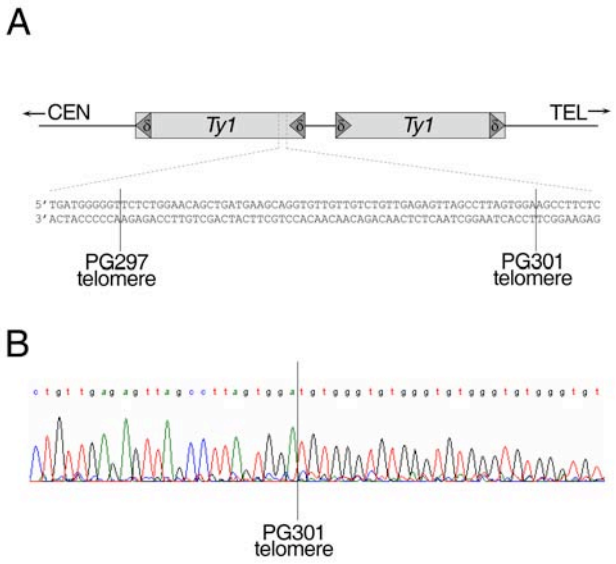

FIGURE S3.—Sequence analysis of two telomere-capped terminal deletions of chromosome III. Three of the illegitimate diploids generated in the *rad52* background had terminal deletions of chromosome III. Using a PCR-based strategy, we determined the breakpoints of deletions in two of the strains (PG297 and PG301). (A) Structure of FS2. The Ty1 elements are represented by light gray rectangles and delta elements by dark gray triangles. Sequences near the 5' end of the centromere-proximal Ty element are shown, with the breakpoints PG297 and PG301 marked with vertical bars. (B) Sequencing analysis of the terminal deletion in PG301. The junction of chromosome III and telomeric sequences is shown as a vertical line.